



TECHNICAL UNIVERSITY OF LIBEREC
Faculty of Textile Engineering ■

AUTOMATIC VISUAL CONTROL SYSTEM FOR TEXTILE PROCESSES

JIRI KULA

SUMMARY OF THE THESIS

Title of the thesis: AUTOMATIC VISUAL CONTROL SYSTEM FOR TEXTILE
PROCESSES

Author: Ing. Jiří Kula
Field of study: P3106 - Textile Engineering
Mode of study: 3103V007 - Textile and material engineering
Department: Department of Textile Evaluation
Supervisor: prof. RNDr. David Lukáš, CSc.

Committee for defense of the dissertation:

Chairman: prof. Ing. Jiří Militký, CSc.	FT TUL, Department of material engineering
Vice-chairman: doc. Ing. Vladimír Bajzík, Ph.D.	FT TUL, Department of Textile Evaluation
prof. RNDr. Gejza Dohnal, CSc. (opponent)	ČVUT Praha, Faculty of Mechanical Engineering,
prof. RNDr. Jan Píček, CSc.	FP TUL, Department of Applied Mathematics
doc. RNDr. Miroslav Brzezina, CSc.	FP TUL, Department of Applied Mathematics
doc. Mohamed F. A. Eldessouki, Ph.D. (opponent)	FT TUL, Department of Textile Technologies
RNDr. Dr. Jiří Janáček	Institute of Physiology CAS, Prague, Biomathematics

The dissertation is available at the Dean's Office FT TUL.

Liberec 2016



Abstract

The work deals with both hardware and software setup of a system dedicated for on-line control of visual quality parameters of fabric. The device is based on aluminum frame, parallel line scan digital cameras and traction mechanism. Related software implementation has been developed as a modular system of independent components, that provide tools like image acquisition, motion control, stitching of images and image analysis. Certain implementation of Gabor filter for description of texture and subsequent texture segmentation has been described. Filters are applied in a new method designed to evaluate dissimilarities between fabric during its quality inspection process. Morphology of Gabor filter is presented both in spatial and frequency domain. Description of planar texture has been treated as a vector of responses of the texture to given bank of filters. Ratio of similarity between two different textures is proposed and also applied in the process of detection of defects.

Keywords: prototype machine, detection of defect, Gabor filter, line scan camera, image stitching, Hotteling control chart, machine learning

Práce se zabývá hardwarovou a softwarovou implementací systému pro on-line kontrolu vizuálních kvalitativních parametrů textilních útvarů. Zařízení sestává z hliníkového rámu, paralelně umístěných řádkových kamer a trakčního ústrojí. Software, který uvedené zařízení ovládá je pojat jako modulární architektura souhry nezávislých komponent. Každá z komponent je odpovědná za dílčí kroky, kterými jsou pořízení obrazu materiálu, kontrola rychlosti posuvu, spojování obrazu z většího množství kamer a analýza obrazu. V práci je obsažen návrh a realizace algoritmu pro rozpoznání viditelné vady materiálu na základě analýzy obrazu pomocí Gaborova filtru, jehož návrh je v práci detailně popsán. Práce přistupuje k detekci vad textilního materiálu tak, že popisuje lokální obraz materiálu pomocí vektoru texturních charakteristik. Rozdíl mezi podobností bezvadného materiálu a materiálu zkoumaného je sledovanou vlastností, která indikuje defekt.

Klíčová slova: prototyp zařízení, detekce defektů, Gaborovy filtry, řádková kamera, panorama obrazů, Hottelingův regulační diagram, strojové učení

Contents

1	Introduction	2
2	Objectives	9
2.1	Hardware implementation	9
2.2	Software implementation	11
3	Pinhole and line scan camera models	12
3.1	Pinhole camera	12
3.2	Linescan camera	12
3.3	Stitching line-scanned images	14
4	Image processing	19
4.1	Gabor filter	19
4.2	Effect of Gabor filter on periodic structure	22
4.3	Similarity of textures	26
4.4	Getting to know defect free texture	29
4.5	Detection of defect	31
5	Experiment	37
5.1	Thin place	39
5.2	Irregular weft density	40
5.3	Broken warp yarn	41
5.4	Yarn defect	42
5.5	Harness misdraw	43
5.6	Hole	44
5.7	Stain	45
5.8	Snag	46
6	Conclusion	48
7	References	50
8	Author's publications	54
9	Published papers	56
10	Unpublished papers	58

1 Introduction

There have been many ways introduced in the development of automated system for quality evaluation of fabric properties. In textile industry, one can most often see an inspection of fabric being done manually. The manual process involves a human operator to watch the surface of material and mark faulty areas by hand. Advanced loom machines are able to detect certain faults by themselves, however, there is still significant amount of defects that need to be inspected after the weaving has been completed. Those defects, that can not be detected on the loom, are particularly certain variations in the appearance of the product. Defects like broken pick or coarse yarn are sorts of defects that can be detected directly on the loom. Those defects like appearance fault, a stain, a hole or a weft kinks, belong to class of defects that remain unnoticed by any other systems than the visual. Gabor filters have proved to be suitable tool for texture description and segmentation [1] when applied in image processing tasks. Approach of tuning filter's response to specific kind of defect called supervised inspection was proposed by Kumar and Pang [2]. The supervised inspection is related to the situation in which the filter response to image of the defect and the material is known a priori. Authors also present unsupervised inspection process, that seems to be more relevant for industrial purposes. During unsupervised inspection, a set of different filters is applied to the local region of image in the manner of multichannel processing. The response of each filter is not known a priori for certain material and defect. Therefore, the training and inspection stages are involved. Another utilization of Gabor filters was proposed by Ro et al. [3] for content description of digital video recordings and searching within this kind of data. This contribution shows an analogous approach in which the similarity between local texture and the reference texture is evaluated. Besides the inspection phase, this work introduces unique principle of multiple line scan cameras acquisition. Also the architecture of custom prototype machine is explained as well as the software that allows to run the inspection algorithm on-line.

The motivation behind existing research in detection and classification of defects of textile structures is driven by issues which the manufacturing process needs to resolve. These are costs associated with time needed to detect and remove fabric defects, money spent on training and salaries of inspectors, and customer satisfaction with the product. Quality management increases the cost [4] of production by 30-50 percent. Weaving is relatively slow process during which about 0.5 meters of fabric is produces per minute. Allocating a human inspector to perform on-line inspection would be costly. Therefore, inspection is performed by unrolling material after the weaving process completes; the off-line inspection. On the other hand, production speed of non-woven textiles can exceed hundreds of meters per

minute in length and up to a few meters in width. A human inspector is not capable to watch for details and evaluate quality of material on-line in this case. Another deficiency of traditional inspection stands in subjective perception of a defect, which varies between individual inspectors, even within one inspector in time.

Visual inspection of material can be generally split into two categories. One category deals with materials that exhibit visually uniform features. Inspection of such materials can be based on monitoring deviation of local image from image background. This category makes use of classic image segmentation methods which are based on edge detection, brightness and color thresholding. These traditional image processing techniques are well mastered and easily adaptable to particular manufacturing process. Examples of typical applications include a blister packaging control in pharmaceutical industry [5, 6] and assembly of components in electronics industry [7, 8]. Another category of material inspection deals with textured materials, which can either be patterned, random or uniform textiles. Patterned textiles have printed motifs or repeated decorations made on jacquard loom. The approaches to inspect textiles of this kind include symmetry assessment, feature registration, matching of primitive spatial patches and model based methods [9, 10]. Quality features of randomly textured textiles, represented with non woven materials, are mostly evaluated in terms of fiber orientation or material homogeneity. Methods based on evaluation of fiber orientation look at details of non woven structure and utilize spectral approach which includes wavelet decomposition [11, 12] and anisotropic bandpass spectral filters [13]. The overall material homogeneity approach represents less detailed look at inspected material, which is suitable to inspect large surfaces. Inspection of large surface can be based on measuring amount of transmitted light through inspected material [14] which finds its application during massive production of disposable, hygienic and geotextile products. Many state of the art inspection systems are proprietary, commercial, and therefore, unpublished solutions.

One of early published assemblies of machine for automatic visual inspection of textiles dates to 1992, when Tincher et al. designed complete machine to evaluate color and shape of a cut material to match required dimensions and ensure defect free workpiece before sewing process [15]. Tincher's solution involves an area scan camera. The methods include segmentation of intensity deviation from image background, and gray level comparison with defect free sample, performed with image subtraction. Even with limited computing power, authors have considered to use spectral approach with the Fourier transformation. Interestingly their conclusion was that spectral approach brings no added value to material inspection. Compared to that investigation, authors found morphological image

operations more suitable. Similar approach to that of Thinché's have been chosen by Norton and Wayne [16] to inspect rolls of web textile fabric in real time. Their method was also based on detecting high contrast defects with bi-level thresholding of each image pixel. The processing has mostly been done with single image pixel at a time. Later research makes use of larger pixel neighborhood processing, which utilizes gray level statistics in image patches and convolution with smoothing kernels [17]. Tolba et al. used autocorrelation function for defect localization and shallow neural network for its classification into five classes [18]. Comprehensive research has been made on texture classification, where majority of papers take co-occurrence matrix as reference to compare novel feature extraction methods. Although important studies concentrate on general texture segmentation, the methods and findings have been later adopted for inspection of textile materials. In-depth description and design of Gabor filter and its application to texture segmentation has been proposed in 1990 by Bovik et al. [19]. Authors identified that filter has great potential for texture segmentation but found the method computationally demanding. Strand and Torfinn in [20] selected textures from Brodatz image database [21] and compared Gabor filter with selected Haralick features [22] (angular second moment, contrast, correlation, entropy) to conclude that Haralick features (computed on co-occurrence matrix) provide lower miss classification error rate, which is 10-20%, compared to 30-50% for Gabor filter in their experiment. Although the Brodatz database contains images of woven and knitted fabric, it also has images of wood, sand and other kinds of natural images. The paper considers tradeoff between sub image size and accuracy of detecting texture boundary. The size of sub windows is 32x32 pixels in their study. While constant window size is claimed in many papers, it is important to note that correct choice of window size shall depend on ratio between image resolution (combination of camera intrinsics with extrinsic setup) and highest spatial frequency present in the image of inspected material. Texture segmentation utilizing Gabor filter has still gained popularity. Weldon and Higgins [23, 24] achieved 4-10% error rate using Bayes classifier and by smoothing the decision of the classifier with morphological erosion followed by dilatation i.e. morphological opening. By morphologically opening the classifier's decision, the authors reduced the number of narrow, misclassified regions. The problem with computational complexity of Gabor filters has been addressed by Teuner et al. [25] by using pyramid approach, which omits filters at lower pyramid levels (high resolution) that have equivalent response with filters in higher pyramid level (low resolution). The method that leads to reduced misclassification error rate, proposed by Weldon and Higgins [23, 24], was an ad hoc solution, which is generally inappropriate. Generalized approach to fine tune a set of Gabor filters for the task to separate a pair of different textures was given by Dunn and Higgins [26, 27]. At the end of the decade, there was no consen-

sus whether statistical texture description methods outperform spectral filtering when Randen et al. [28] provided review of Gabor filter banks, wavelet transforms, discrete cosine transformation and compared them to co-occurrence matrix and autoregressive features. Authors concluded that the accuracy of classification among selected methods is dependent on particular type of texture, and single method can not be declared better than other methods.

The approach to define textile material inspection as a texture segmentation task was chosen in several papers. Bodnarova et al. [29] has shown accurate flaw detection with low false alarm rate on woven textiles and suggest optimization of Gabor filters with non-linear programming to deal with more complicated problem of detecting flaws in jacquard textiles. Bodnarova's work, however, does not address construction of inspection machine, as well as problems associated with image acquisition. Kumar and Pang [30] propose to select single filter from a bank of filters. Authors have developed heuristic algorithm to select the filter which has the greatest response on particular defect in given textile. Material inspection is understood in their work as supervised and unsupervised learning approach in two chapters. In both chapters, defect free texture is learned, or defined, with the filter which has maximum response on given texture. Authors consider computational demands of multi channel processing with a bank of Gabor filter, which is the motivation behind selecting only one filter. Although Kumar and Pang did not design an inspection machine, they suggest using a digital signal processor (DSP) to perform multi-channel processing with entire bank of filters. Selecting a single filter restricts their method for very limited variations in size, shape and orientation of particular defect which, under real conditions, yields rather low accuracy of detection. Textures in the article are images of woven fabric and method of dividing entire image into smaller sub-windows has been used. The method of searching for single filter introduced by Kumar and Pang have inspired Han and Zhang [31], who proposed fine tuning of the filter using genetic algorithm. The principle of their method is to find the closest match between the filter and image of particular defect free woven fabric. Performance of their method reached 92% true positive rate.

Complete system for quality inspection of textiles has been realized in 2000 by Baykut et al. [32], who evaluated statistical, spectral and model based methods on images of woven fabric manufactured in Turkey. Their method based on Markov random fields, using relatively straightforward statistics over neighboring pixels, over performed co-occurrence matrix and Fourier spectrum energy for their training set of images. Authors have designed and assembled inspection machine to capture surface of 1.6 meter wide textiles using four CCD area scan cameras. Image processing has been done on embedded hardware using DSP, which allowed to

inspect ten meters of material per minute. Real inspection system, making use of more demanding spectral approach with Gabor filters, has also been implemented by Mak and Peng in 2006 [33], who performed inspection in laboratory conditions to achieve 96% true positive rate on publicly available database of images containing defects of textile fabrics. Inspection machine has been assembled with single line scan camera. Although authors achieved the velocity of 15 meters per minute, the width of captured material has been merely a few centimeters. In 2011, Yao and Hai-ru [34] published their study on hardware implementation of inspection device, mounted on existing inspection machine to perform inspection of defects in knitted textiles. Inspection system has targeted three categories of defects: a hole, a dropped stitch and a course mark. Authors developed two distinct detection algorithms. Detection of a course mark defect has been made with Ridgelet transform. The defect of hole and dropped stitch have been detected with pulse coupled neural network.

The opportunity to engage Gabor filters in material inspection of textiles has been explored, and reasonable number of complete inspection systems has been designed. Still there is no consensus regarding inspection performance of particular algorithm with certain type of textile material. Publications such as [32] are evidence that real time implementation system utilizing computationally demanding algorithm can be accomplished. Although, in that case, the real time performance has been achieved with excessive effort put into particular DSP implementation, which provides low flexibility. No scientific work has been published in the field of textile fabric inspection which deals with image acquisition itself to great level of detail. Location of defects is usually provided in image coordinate space, i.e. the image pixels, which is inappropriate for practical use. Camera calibration, the effect of line scan imaging on image deformation, the stitching of images from array of line scan cameras, represent uncovered aspects of visual inspection system designed to satisfy the needs of textile industry and the needs of researchers to concentrate on the algorithm itself and not the device that it runs on. None of the published implementations provide a framework. A modular, multi layer system, which would solve repetitive technical problems and which would provide environment to plug the algorithm into the image processing pipeline in convenient manner. Experience shows that there can be a significant degradation in ability of particular algorithm to detect defects in textiles whether it runs under simulated and real-world conditions. This work aims at covering problems stated above, which were not given sufficient attention in scientific publication. The dissertation also deals with the design of inspection machine and associated software framework that allows running of virtually any visual inspection method. The high level design is particularly different from other implementation, in that it provides enough flexibility to extend. Functionality of the system has been demonstrated by

implementing the inspection algorithm that makes use of spectral approach with Gabor filters. The dissertation not only uses Gabor filters that were considered suitable for visual inspection of textiles, but it also aims at describing reasons for effectiveness of the method. Importance of image pre-processing, which needs to be taken before a bank of Gabor filters can be applied, is underlined and considered as possible reason for failure of Gabor filters in other publications.

The dissertation represents natural step in long term development of automatic visual control system for textiles, and results achieved throughout this dissertation extend capabilities of continuing research in the field. Among research activities conducted on Technical University of Liberec can be recognized works of Tunak and Linka who have dealt with stochastic simulation of textile structures [35], statistical and spectral methods for automatic evaluation of weaving density on the loom [36], directional defects of woven textiles [37, 38], quality assessment of non-woven structures [39] and yarns [40], in which the inspection device presented inhere, has played significant role in image acquisition and evaluation of novel concepts in real-world environment.

The first section serves as an introduction to the field and a survey of visual control systems for textile structures.

The second section states objectives of this work and strategies selected to fulfill them.

The third section describes models of a pinhole and a line scan camera. The geometry of image acquisition with line scan camera is explained to great detail. The camera model plays important role in understanding of how an image of a line scan camera is acquired. Since the scene and camera position in the scene influence how objects appear in the image, it is crucial to understand world to image coordinate relations in order to rectify image distortion as well as to stitch images of multiple cameras into single large panoramic image. Stitching of multiple line scan images is the first of the two key concepts presented in this work. The ability to deal with multiple sources of image data is essential for the reason that the field of view of a single camera is generally not sufficient to cover large surface of material produced in typical textile manufacturing process.

The fourth section deals with image data itself. This section explains morphology of the Gabor filter in great detail. the effect of the filter on woven fabric is shown and the perfect match between properties of the filter and structural properties of woven textiles is uncovered. The key concept in this section is that image of textile fabric is assumed to represent a texture. The inspection algorithm is built on comparison between texture of the flawless and the inspected sample. Design of the Gabor filter is shown and approach to handle large image of textile material

is explained in detail.

Experiments are presented in the fifth chapter, which includes discussion about classification performance as well as difficulties that each kind of defect represents to the inspection method. Because Gabor filters are still computationally demanding, the discussion suggest for performance optimization.

2 Objectives

The work can be divided into four parts.

- Design and build prototype machine for inspection of moving textile material in order to simulate production environment in laboratory.
- Acquire image of textile material loaded in prototype machine.
- Evaluate visible flaws of the material by means of image processing.
- Provide software that deals with machine control, image acquisition and image processing aspects of the whole system.

2.1 Hardware implementation

A model of designed machine is illustrated in Figure 1a. The model on the left does not show begin and end of material, which suggests the process of continuous inspection. The photography in Figure 1b shows that material is actually made of endless belt of fabric that is drawn between two rolling drums.

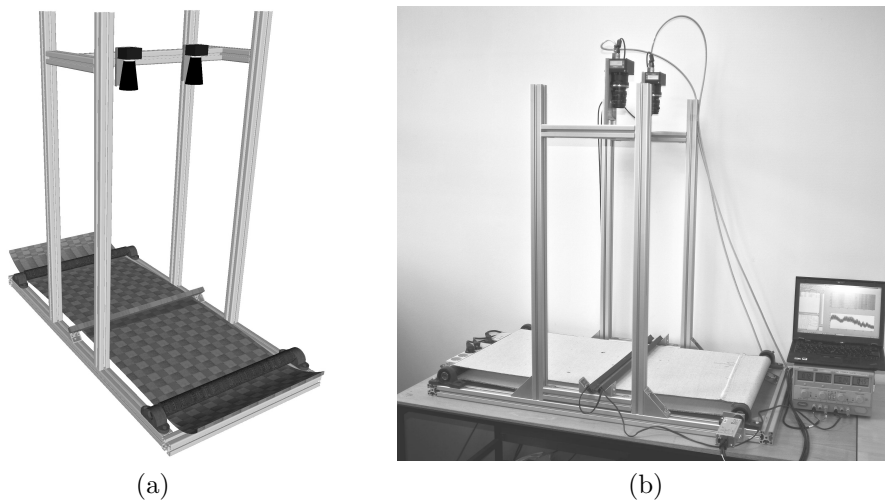


Figure 1: Prototype machine to perform on-line detection of visual flaws of textile material; (a) 3D model of inspection device; (b) photography of actual prototype machine.

Schematic outline of the device can be seen in Figure 2. The device is made of aluminum frame. Base of the frame holds two rolling drums among which is tightened

an endless strap of fabric. One of rollers is driven with Maxon MCD EPOS 60W electric motor. The motor is controlled by software. Embedded encoder provides information about current position and velocity. This information is utilized for synchronization of cameras as well as for registration of incidental defect's position. Another necessary equipment is LED light array, spanned across fabric's width, positioned in the middle between two rollers. The light array provides stable illumination of portion of fabric that is acquired with two line-scan cameras Basler L401k. Cameras are positioned in the upper part of machine above inspected material. They are oriented down so that field of view (*FOV*) of each camera includes illuminated portion of fabric. Each camera has an array of *4080* pixels and provides gray scale image. The width of fabric belt is *500* mm, which is actually within *FOV* of a single camera. However, the reason for using two cameras is to face and solve the problem of synchronizing multiple image sources and merging them into a single large image - the concept that would be necessary during actual production, where the width of fabric reaches up to few meters.

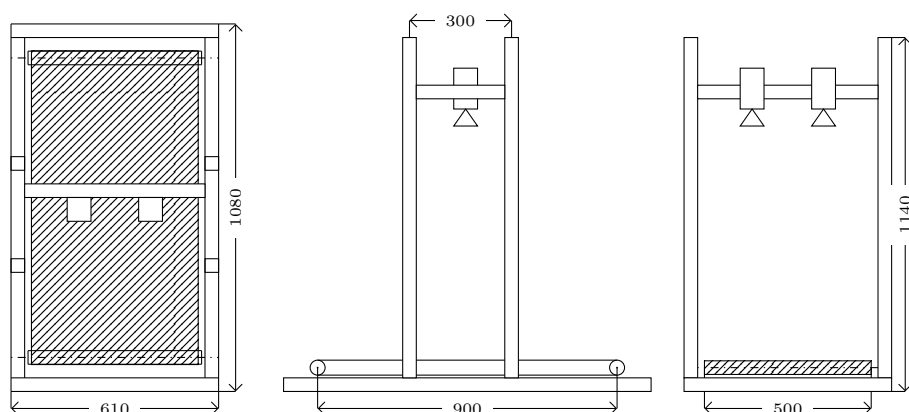


Figure 2: Inspection device schematic. The figure shows the top, side and front view of inspection device. It also depicts positions of two line scan cameras, whereas driving unit and light array are not shown in the schematic view. Dimensions are given in millimeters.

The device is controlled with ordinary personal computer, equipped with *CameraLink* expansion card. The *CameraLink* interface is used to connect cameras, while motor is connected through standard serial interface. The image in Figure 1b also captures laboratory power supply and laptop computer that is not attached to the device but it presents status information provided by control software. It is a feature of software solution that it is able to form distributed system in which image acquisition and processing can be done on different computers.

2.2 Software implementation

As well as custom hardware, a custom software has been developed. The software solves these tasks:

- Hardware synchronization between belt velocity and line scanning frequency.
- Image acquisition.
- Image processing and presentation of results.

The software is a Windows application that hosts independent software components, making it open for further extension through plug-ins. Every plug-in, or component, shows itself as a block in a graph. Components connect through their input and output interfaces, thus forming complete topology of operations. Underlying technology is *DirectShow*.

The application is not a single, monolithic piece of software but a platform that can include another, future components without change in its source code. It has been expected that not a single image processing component, presented in current state of the work, would suffice for every kind of textile material. For that reason, any stage in the graph can be exchanged while keeping other aspects, like image stitching, with no modification.

3 Pinhole and line scan camera models

In this section, a pinhole camera and a line scan camera models are described. Camera and image acquisition are tightly related areas of image processing. Fundamental aspects of image acquisition with line scan camera is derived from pinhole camera model.

3.1 Pinhole camera

The work explains pinhole camera model as linear mapping between world and image points as follows.

$$\mathbf{x} = \begin{bmatrix} \alpha_x & s & x_0 \\ 0 & \alpha_y & y_0 \\ 0 & 0 & 1 \end{bmatrix} \begin{bmatrix} r_{11} & r_{12} & r_{13} \\ r_{21} & r_{22} & r_{23} \\ r_{31} & r_{32} & r_{33} \end{bmatrix} \begin{bmatrix} 1 & 0 & 0 & -C_x \\ 0 & 1 & 0 & -C_y \\ 0 & 0 & 1 & -C_z \end{bmatrix} \begin{bmatrix} X \\ Y \\ Z \\ 1 \end{bmatrix} = \mathbf{KR}[\mathbf{I} \mid -\mathbf{C}]\mathbf{X}$$

$$\mathbf{P} = \mathbf{KR}[\mathbf{I} \mid -\mathbf{C}] \tag{1}$$

where \mathbf{P} represents internal camera parameters $\alpha_x, \alpha_y, s, x_0, y_0$ together with external camera parameters \mathbf{R}, \mathbf{C} of general pinhole camera.

3.2 Linescan camera

Pinhole camera is a model of area scanning camera. Area scan camera acquires an image of a scene that fits inside camera's field of view. The field of view of area scan camera is limited by objective properties relative to width and height of the sensor. The sensor is made out of cells arranged into two dimensional matrix - into rows and columns of semiconductors sensitive to light. Another camera exists, called line scan camera, that features only single row of detectors. Line scan camera captures along single dimension at a time. The field of view of a line scan camera is limited to single line segment, so that it's image has resolution of $width \times 1$ pixel, where $width$ stands for number of pixels of a sensor. A camera acquires single line at a time but it is able to acquire at high frequency. Area image is achieved by stacking multiple lines consecutively. The requirement here is that either a scene or a camera change position between two lines, so that each

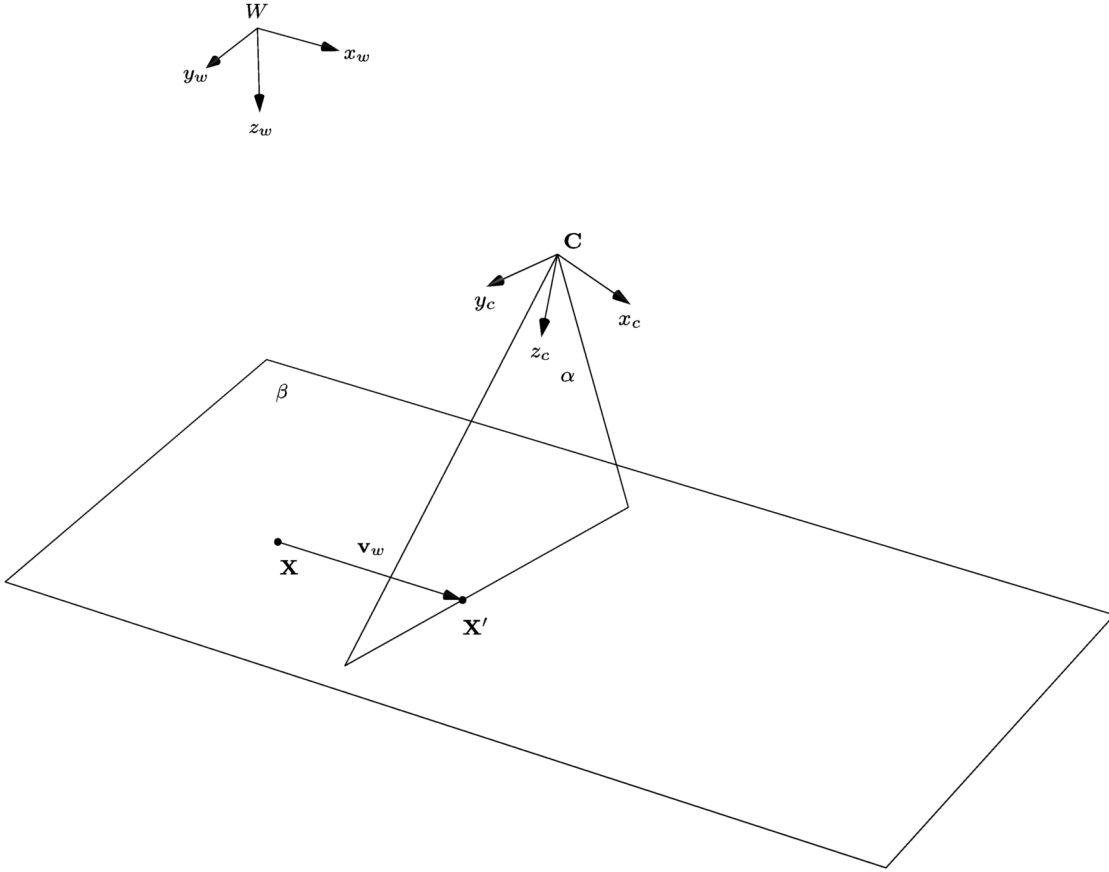


Figure 3: Principle of line-scan camera acquisition. The plane β represents points of planar scene in world coordinate frame, W , that move with common velocity \mathbf{v}_w . One of these points is a point \mathbf{X} . Camera C is placed above the plane β and it is oriented toward it. Camera position and orientation form camera coordinate frame. The camera is line-scan, which implies that it's FOV is limited by single row of pixels at the moment of acquisition. Thus the FOV of camera C forms acquisition plane α . Point \mathbf{X} will be viewed by camera C only at time t when it reaches position \mathbf{X}' . Point \mathbf{X}' lies on a line formed by intersection of acquisition plane α with the scene plane β .

line captures different portion of a scene. Regarding current system, two cameras are static and the material moves.

$$\mathbf{x} = \begin{bmatrix} t \\ \omega u \\ \omega \end{bmatrix} = \begin{bmatrix} 1 & 0 & 0 \\ 0 & f & p_v \\ 0 & 0 & 1 \end{bmatrix} \begin{bmatrix} -1/v_x & 0 & 0 \\ -v_y/v_x & 1 & 0 \\ -v_z/v_x & 0 & 1 \end{bmatrix} [\mathbf{R} \quad -\mathbf{RC}] \begin{bmatrix} X \\ Y \\ Z \\ 1 \end{bmatrix} = \mathbf{MX} \quad (2)$$

3.3 Stitching line-scanned images

Linescan camera pose results in image distortion. Figure 4 presents example of scanning a chess with two linescan cameras in general position. Image of camera on the left, \mathbf{L} , and camera on the right, \mathbf{R} suffer mainly from shear deformation due to camera rotation around z axis. Approach to combine image of camera on the left with image of camera on the right is as follows.

The chess moves with velocity $\mathbf{v}_w = (v_x, 0, 0)^T$. Assumption is that optical centers of two cameras have the same Z_ω coordinate and equivalent intrinsic parameters \mathbf{K} . If cameras also had the same rotation matrix $\mathbf{R}_L = \mathbf{R}_R = \mathbf{I}$, then stitching could be done with simple translation. The translation of, let's say, right camera to the image of left camera would stitch the two images into complete view of entire object. In fact it is not possible to mount both cameras unrotated with respect to world coordinate frame. The strategy is to undistort image of real camera as if it came from the camera whose rotation was an identity matrix. Then, translate image of the right camera, \mathbf{R} to merge to image of the left camera \mathbf{L} .

Having 3×4 linescan camera matrix \mathbf{M} , camera intrinsic and extrinsic parameters can be recovered with QR decomposition, see Appendix A. Decomposition reveals parameters of chess velocity in camera coordinate frame, \mathbf{v}_c , camera rotation matrix \mathbf{R} and intrinsic parameters matrix \mathbf{K} . Combining these three parameters, a 3×3 matrix \mathbf{N} can be found that maps image of real camera to image of unrotated camera as follows.

$$\mathbf{N} = \mathbf{KQ}(\mathbf{KSR})^{-1} \quad (3)$$

The velocity vector \mathbf{v} in world and unrotated line scan camera coordinate frames are identical. It is recovered from camera matrix \mathbf{M} as well as \mathbf{K} and \mathbf{R} are.

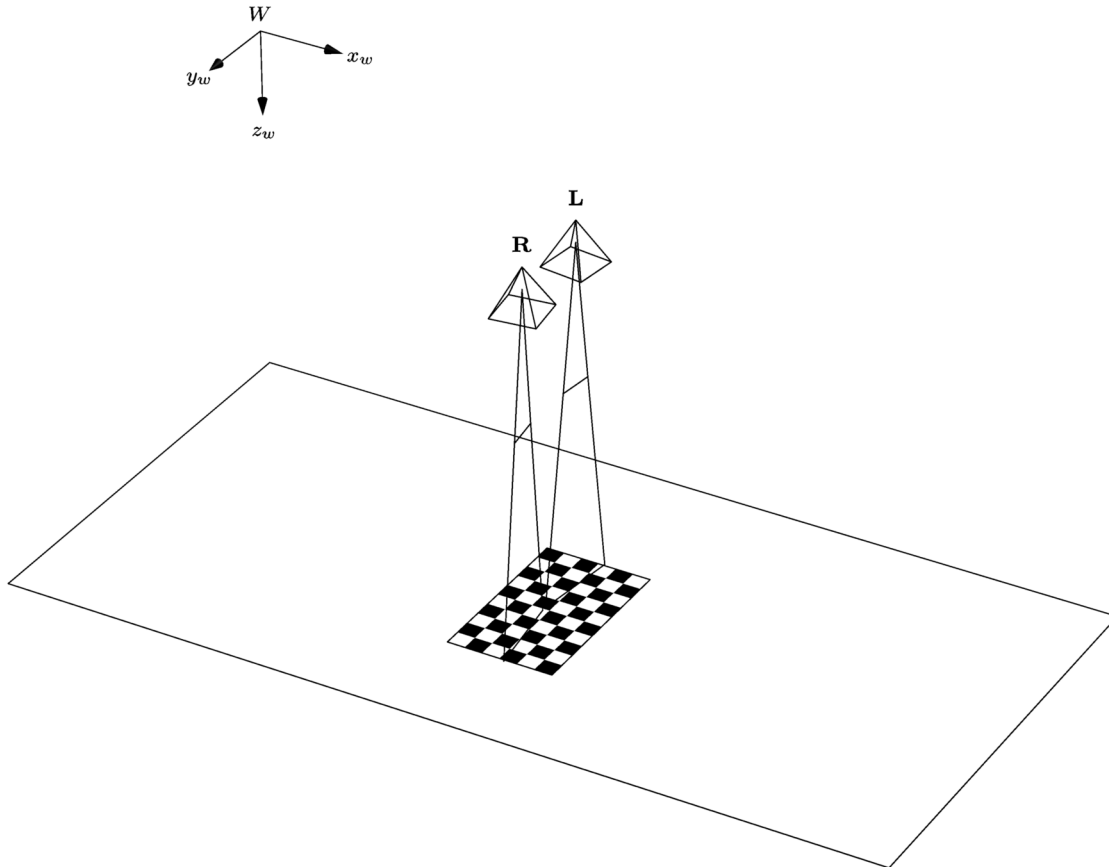


Figure 4: Image acquisition with two line-scan cameras. Camera \mathbf{L} and \mathbf{R} have unique position and orientation in world coordinate frame \mathbf{W} . Acquired feature, the object, is a chess. The chess is a grid of alternating white and black fields. Intrinsic and extrinsic parameters of both cameras are constant in time, while the chess moves. The chess here is simply to illustrate a set of points on a world plane, see Figure 3.

$$\mathbf{v} = \begin{bmatrix} v_x \\ v_y \\ v_z \end{bmatrix} = \mathbf{R}^T \mathbf{v}_c \quad (4)$$

$$\mathbf{Q} = \begin{bmatrix} -1/v_x & 0 & 0 \\ -v_y/v_x & 1 & 0 \\ -v_z/v_x & 0 & 1 \end{bmatrix} \quad (5)$$

The matrix \mathbf{S} represents chess velocity matrix in camera coordinate frame.

$$\mathbf{S} = \begin{bmatrix} -1/v_x^c & 0 & 0 \\ -v_y^c/v_x^c & 1 & 0 \\ -v_z^c/v_x^c & 0 & 1 \end{bmatrix} \quad (6)$$

Homogeneous coordinates of an image point is of a form $\mathbf{x} = (x, y, 1)^T$. The ω coordinate, see equation 2, is missing from the image. It can be found from known camera matrix \mathbf{M} as follows. The i -th and j -th element of \mathbf{M} is denoted m_{ij} .

$$\begin{aligned} a &= m_{31} - \frac{m_{32} \cdot m_{11}}{m_{12}} & e &= m_{21} - \frac{m_{22} \cdot m_{11}}{m_{12}} \\ b &= \frac{m_{32}}{m_{12}} & f &= \frac{m_{22}}{m_{12}} \\ c &= \frac{m_{32} \cdot m_{14}}{m_{12}} & g &= \frac{m_{22} \cdot m_{14}}{m_{12}} \\ d &= m_{34} & h &= m_{24} \end{aligned}$$

$$\begin{aligned} X &= \frac{f \cdot x - b \cdot x \cdot y + (c - d) \cdot y - g + h}{a \cdot y - e} \\ Y &= \frac{1}{m_{12}} \cdot (x - m_{11} \cdot X - m_{14}) \\ \omega &= m_{31} \cdot X + m_{32} \cdot Y + m_{34} \end{aligned}$$

After ω is found for image points \mathbf{x} and stored as \mathbf{x}_ω , the image distortion can be undone with unrotation matrix \mathbf{N} into undistorted coordinates \mathbf{y} .

$$\mathbf{x} = \begin{bmatrix} x \\ y \\ 1 \end{bmatrix} \quad \mathbf{x}_\omega = \begin{bmatrix} x \\ \omega y \\ \omega \end{bmatrix}$$

$$\mathbf{y} = \mathbf{N}\mathbf{x}_\omega \quad (7)$$

These are related only by translation, which can be obtained from pair of respective unrotated camera matrices. Having two linescan cameras \mathbf{M}_L , \mathbf{M}_R and their unrotated versions \mathbf{L} , \mathbf{R} , obtained from equation 3, as

$$\mathbf{L} = \mathbf{N}_L\mathbf{M}_L \quad \mathbf{R} = \mathbf{N}_R\mathbf{M}_R \quad (8)$$

translation parameters are extracted from \mathbf{L} and \mathbf{R} as follows.

$$\begin{aligned} f^l &= L_{22} & f^r &= R_{22} \\ t_x^l &= L_{14} & t_x^r &= R_{14} \\ t_y^l &= L_{24} & t_y^r &= R_{24} \\ t_z^l &= L_{34} & t_z^r &= R_{34} \end{aligned}$$

Translation matrix \mathbf{T} is in the form

$$\begin{aligned} t_x &= t_x^l - t_x^r \\ t_y &= \frac{f^l \cdot t_z^r}{f^r \cdot t_z^l} - \frac{f^l \cdot t_y^r}{f^r \cdot t_z^l} + \frac{t_y^l}{t_z^l} \\ \mathbf{T} &= \begin{bmatrix} 1 & 0 & t_x \\ 0 & 1 & t_y \\ 0 & 0 & 1 \end{bmatrix} \end{aligned} \quad (9)$$

Let's denote points of the left unrotated camera image \mathbf{y}_l and points of the right unrotated camera image \mathbf{y}_r . Image points of stitched image, containing image of both cameras are \mathbf{y}_s . Left camera points are copied into stitched image with no change, while image of camera on the right are translated by \mathbf{T} .

Ideally, right camera field of view begins exactly where left camera field of view ends. In reality, cameras are set so that their images overlap and portion of a

scene is visible in both cameras. Following two equation are symbolic and mean combination of the two images into single panoramic image \mathbf{y}_s .

$$\mathbf{y}_s = \mathbf{I}\mathbf{y}_l \quad \text{and}^1 \quad \mathbf{y}_s = \mathbf{T}\mathbf{y}_r \quad (10)$$

Approach described above has disadvantage in the need to calibrate each camera and advantage that fields of view of cameras needs not overlap much to get panoramic image. It also applies, that each world point, i.e. location of defect, is known directly from it's image.

¹The *and* means interpolation of intensity to achieve soft joint between two images; a technique known as panorama or image mosaicing.

4 Image processing

While preceding section considered formation of image with line scan camera, section 4 concentrates on content captured in the image and what information can be extracted from its pixels.

Majority of fabrics consist of two perpendicular yarns. The way these yarns are woven gives the final product a specific texture, or a pattern that is infinitely repeated over the area of fabric.

Digital image can be thought of as discrete function f spanned across two dimensional vector $\mathbf{r}^* = (x, y)^T$, where $(x, y)^T$ express a point of the image plane in spatial coordinates. From the perspective of spectral analysis, the image of textile structure can be considered as two dimensional, discrete and periodic signal.

Following are key ideas of this section.

- Image of woven fabric captures periodic signal.
- Perform analysis on image in frequency domain using Gabor filter.
- Consider filter response as feature of fabric at particular frequency band and orientation.
- Detect visible flaw of material by comparing features of perfect and defective textures. Use Hotelling T^2 statistics in order to compare features of material.
- Area of woven fabric is so large that it's image can not even fit into computer memory. How to deal with local image processing.

Image processing section begins with structure of Gabor filter and generation of set of filters. This set, or a bank of filters, is then applied to image in order to reveal features of textile material. It will be shown how bank of filters can break complex image down to it's fundamental components. After decomposition, application of Hotelling T^2 statistics on image features will be explained. A classification performance measure, the ROC curve, has been used to estimate classification for various upper control limits.

4.1 Gabor filter

Gabor filter in spatial domain is two dimensional Gaussian modulated with a harmonic function. The Gaussian part has three parameters; the orientation of filter with respect to image coordinate system, the extent along filter's x, y axes and position of filter within image plane. The extent of the filter, σ_x, σ_y , is expressed

with 2×2 matrix $\mathbf{s} = \begin{pmatrix} \sigma_x & 0 \\ 0 & \sigma_y \end{pmatrix}$ of standard deviations. Orientation is expressed with 3×3 rotation matrix \mathbf{R} . The location is captured in the 3×3 translation matrix \mathbf{T} . The second part of Gabor filter, the harmonic function, has properties of frequency ω and orientation. The orientation of harmonic function matches the orientation of Gaussian here.

$$G(\mathbf{r}, \mathbf{s}, \mathbf{t}, \omega) = e^{\left(-\frac{1}{2}\mathbf{r}^T\mathbf{s}^{-1}\mathbf{r}\right)} \cdot e^{(\omega\mathbf{t}^T\mathbf{r})}, \quad (11)$$

where \mathbf{r}^* means point in image coordinate space, $\mathbf{r} = \mathbf{R}\mathbf{T}^{-1}\mathbf{r}^*$ means image point in filter coordinate space. The \mathbf{t} stands for direction of filters x_f axis with respect to image x_i axis, which is first column of the matrix \mathbf{R} . Linear transformations are carried out in homogenous coordinates.

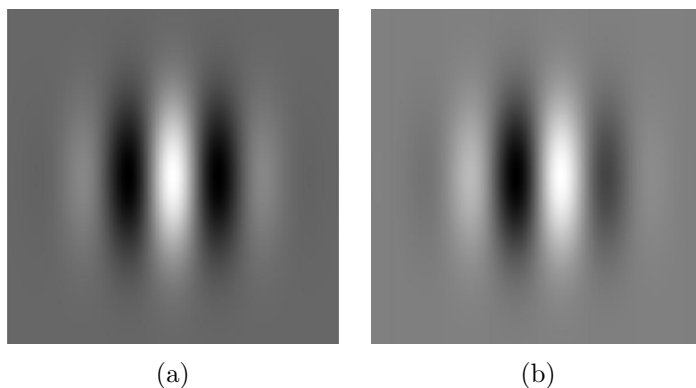


Figure 5: Gabor filter in spatial domain; (a) real part, (b) imaginary part. The filter is combination of two dimensional Gaussian and harmonic function. The filter in spatial domain forms a convolution kernel. It can be used to enhance edges in vertical (presented here), horizontal or arbitrary orientation.

Gabor filter can be also defined in frequency domain using polar coordinates (Ω, Θ) . Vector \mathbf{s} would have a meaning of extent of the filter along axial and radial direction $\mathbf{s} = (s_\Omega, s_\Theta)^T$. The diagonal matrix $\mathbf{R} = \begin{pmatrix} \omega-\Omega & 0 \\ 0 & \theta-\Theta \end{pmatrix}$ represents the distance from the center of the filter, where $\Omega = (\mathbf{r}^T\mathbf{r})^{\frac{1}{2}}$, $\Theta = \arctan(\frac{y}{x})$ stand for transition of Cartesian coordinate \mathbf{r} into polar coordinate (Ω, Θ) . Filter in frequency domain is given by equation 12.

$$G(\Omega, \Theta) = e^{-(\mathbf{s}^T\mathbf{R}\mathbf{R}\mathbf{s})} \quad (12)$$

Gabor kernel in frequency domain is a bandpass filter. The principle of using filters in frequency domain consists of multiplication of spectrum of input image by a set

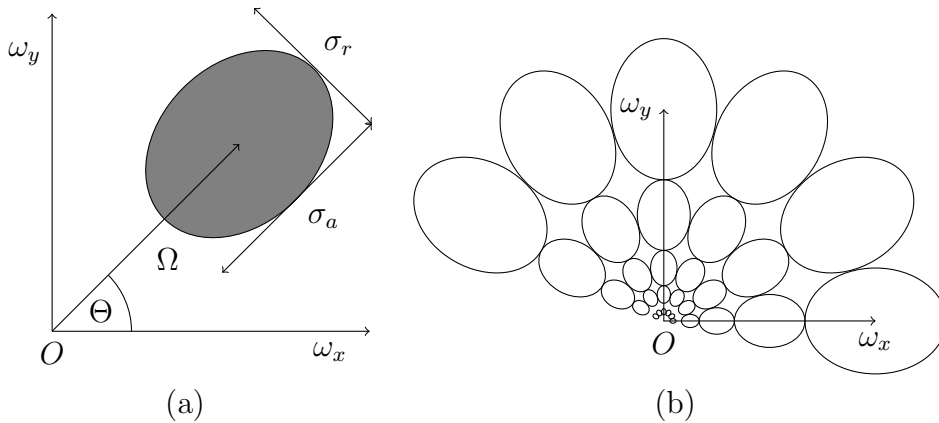


Figure 6: Design of Gabor filter in polar coordinates; (a) only the first quadrant of frequency space is visible, so that O is placed at the center of frequency space; (b) the frequency space is distributed into multiple channels with a set of filters.

of (non overlapping) kernels that together cover the entire area of the spectrum. Filters are, as a rule, build such that each filter covers single octave band of the frequency spectrum. The frequency representation of spatial image is obtained by Fourier transformation with DC component shifted to the center of frequency space. It is appropriate to carry out the design of kernels in polar coordinates, which is consistent with the previous definition of the filter in equation (12).

Filters, like the one shown in Figure 6, are constructed to cover the whole frequency space. Each of filters extracts a portion of information from the image, or spectrum of the image respectively. There is considerable redundancy in information when adjacent filters overlap [41], which can be reduced by means of following filter design. Radial (angular) bandwidth σ_{Θ} is a constant value for the entire set of filters. Axial bandwidths of filters are set one octave wide depending on distance Ω of the filter from the origin O . Considering two different frequencies ω_0, ω_1 such that $2\omega_0 = \omega_1$, the distance between these two frequencies is one octave. Let's take the third frequency ω_2 , which is twice as high as the second frequency: $\omega_2 = 2\omega_1 = 2 \times 2\omega_0 = 2^2\omega_0$. The distance between frequencies ω_0 and ω_2 is in the range of two octaves. It follows that the number of octaves k , that spreads between two different frequencies $\omega_{min}, \omega_{max}$, is given by equation (13).

$$k = \log_2 \frac{\omega_{max}}{\omega_{min}} \quad (13)$$

The width of i -th band in axial direction, $B_{a,i}$, equals to its lower frequency limit ω_i , as shown in Figure 7. The center of each filter is placed in the middle of

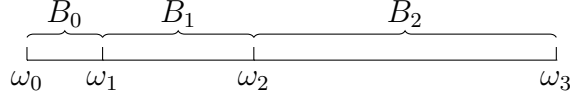


Figure 7: Explanation of octave. Symbols ω_i denote increasing frequency, B_i denote band width of respective octave. Bandwidth B_i which is the width of i -th octave equals ω_i .

i -th octave. In order to avoid redundancy produced by overlapping adjacent filter, their extents are designed so that the neighbouring filters touch at half of their amplitude, which equals to 1 in the center of Gaussian and decreases outwards. Size of standard deviation in axial direction σ_Ω can be derived from Figure 7 as well, where the width of i -th band is denoted B_i . In accordance to previous restriction it means that $e^{-\frac{(\frac{1}{2}B_{a,i})^2}{2\sigma_a^2}} = \frac{1}{2}$. Thus, i -th standard deviation in axial direction is given by $\sigma_\Omega^i = \frac{B_{a,i}}{2\sqrt{\ln(2)}}$. The number of filters, n , at each axial band is a constant. So the extent of each filter in radial direction follows $B_r = \frac{2\pi}{n}$. The size of the standard deviation in the radial direction is therefore a constant as well, $\sigma_\Theta = \frac{B_r}{2\sqrt{\ln(2)}}$.

$$\mathbf{s} = \begin{pmatrix} \frac{2\sqrt{\ln 2}}{B_a} \\ \frac{2\sqrt{\ln 2}}{B_r} \end{pmatrix}$$

Thanks to the symmetry of the Fourier spectrum around its origin, it is good enough to deal with only single half of entire spectrum. At the moment of preparing bank of filters, it is therefore sufficient to generate only the filters at angles between $\langle 0, \pi - B_r \rangle$. Resulting filter bank for $B_r = 30^\circ$ and octave count $k = 7$ is shown in Figure 8.

4.2 Effect of Gabor filter on periodic structure

Gabor filter has the property that it enhances edges of certain width and certain orientation of image. Next figures show effect of various filters on single image of woven fabric. Filters are different in frequency band and orientation that they cover. The Figure 9 shows two images side by side. On the left is spatial image of woven textile. It features horizontal, vertical, and diagonal stripes. Image on the

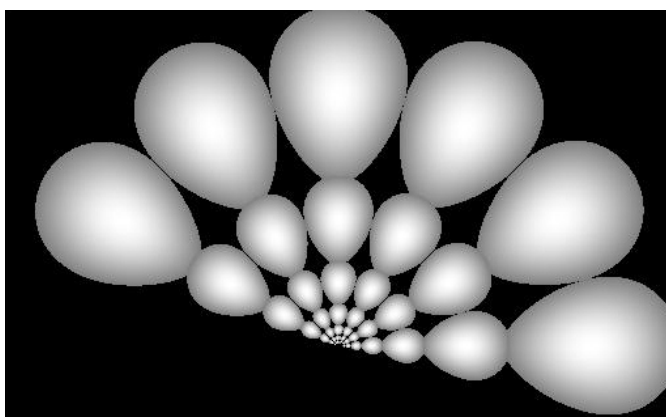


Figure 8: A bank of Gabor filters. This figure shows all the filters integrated into single image. It has been done to show how all the filters, when used together, cover whole frequency space at given frequency bands (octaves) and in various orientations. Each single one of these filters is applied to frequency spectrum of input image one by one, not all the filters together.

right shows frequency spectrum of the image on the left. The spectrum has been shifted to center, so that it's DC component is in the middle of the image.

The Fourier transformation is linear, invertible. It allows to move back from frequency to spatial representation. What happens if the filter is applied in frequency space and then the image is transformed back to spatial domain is shown on Figure 10. Three examples are shown here, each presenting different Gabor filter. The difference between each filter is in frequency that the filter covers. Orientation of all three filters is constant, $\Theta = 0$.

There are five steps involved in producing output shown in Figure 10.

1. Multiply original, spatial, image element by element with 2D Hamming window ².
2. Compute 2D Discrete Fourier Transform (DFT) of windowed spatial image.
3. Generate Gabor filter at particular frequency band (Ω) and orientation (Θ).
4. Multiply frequency plane with filter plane element by element.
5. Take the output of previous step and compute inverse DFT.

The Figure 10 points to important properties of spectrum and filter. The three filters used in example have effect of enhancing vertical edges, which can be un-

²For windowing function, see Appendix B

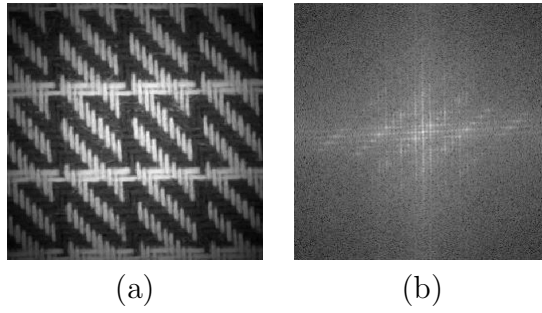


Figure 9: Spatial image of woven fabric with horizontal, vertical and diagonal stripes, (a), and its discrete frequency spectrum on the right (b). Image and its spectrum have the same number of pixels. Intensity of pixel in frequency space has meaning of amplitude of sine/cosine wave at that particular frequency. The frequency is measured from the center of spectrum, which represents zero frequency.

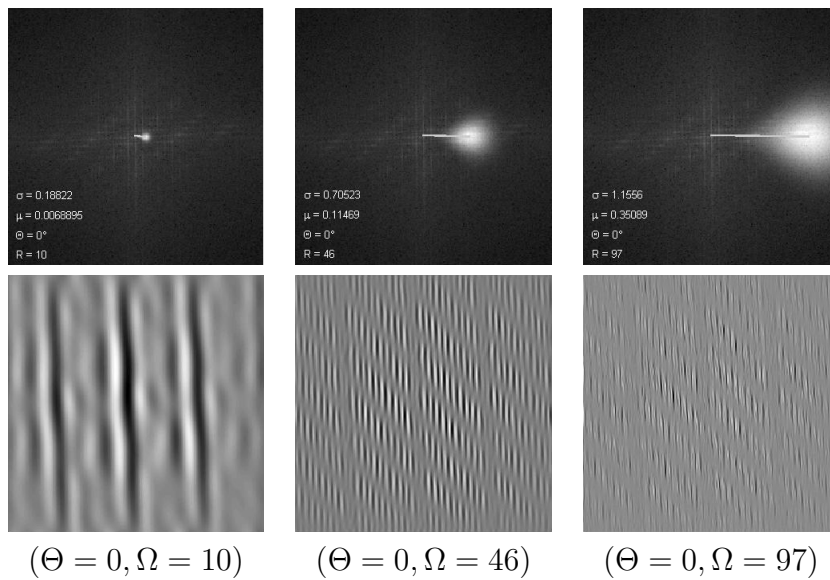


Figure 10: Response of three filters to image of fabric containing apparent directional pattern. Superimposed spectrum with the filter is shown in the 1st row. There is also a radius vector printed on each image that connects the center of the spectrum plane with the origin of the filter (the zero frequency). Pictures below show the inverse Fourier transform of filtered spectrum. The filter posed in horizontal orientation enhances vertical edges of spatial image.

derstood as extracting warp yarns in context of woven textiles. The filter also cuts of those edges, that fall outside filters range. The effect of filter, besides the orientation, depend on frequency band. The filter near center of spectrum works with low frequencies and enhances long periods in image. Filters in higher octaves enhance higher frequency components. When applied to image of fabric, the bank of Gabor filters is good at separating the product down to individual yarns.

- Filter's extent along axial direction restricts it's effect to particular size of feature in spatial image.
- Orientation of filter limits it's effect to perpendicular edges in the spatial image.

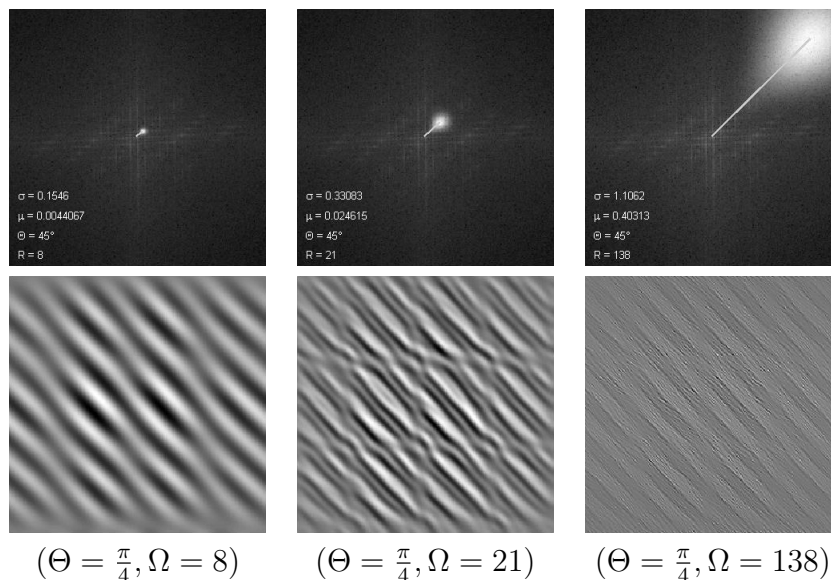


Figure 11: Effect of Gabor filter applied at angle of 45° in three different frequencies. Filter at this configuration rejects vertical and horizontal edges but passes diagonal edges through to the output. Diagonal stripes can be matched to the stripes visible in the original image.

The three examples have shown relatively complex fabric, exposing sharp edges in different directions. Filters that were applied to frequency spectrum of image of such structure can attenuate or emphasize any part of this structure, depending of filter configuration. Using appropriate set of filters, any complex structure can be decomposed into it's underlying components, thus be analyzed.

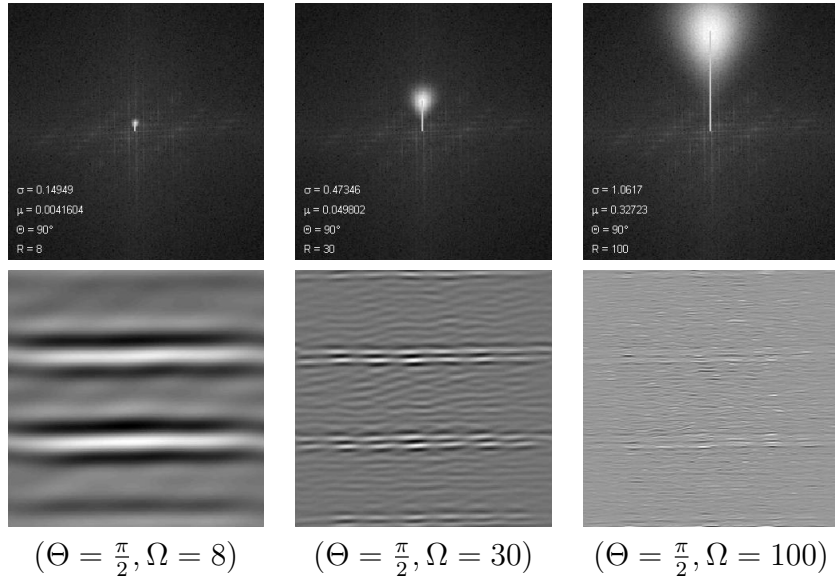


Figure 12: The filter at 90° passes only horizontal edges. It is common that lower frequencies (left, middle) capture real structure while higher frequencies (right image) are badly affected by noise.

4.3 Similarity of textures

In context of detection of visible flaw in textile material, the thesis formulates the problem as a challenge to recognize whether inspected piece of material is different from perfect material. More precisely, whether digital image of inspected material has the same features as image of non-defective structure. If the condition is not met, then the structure does not meet required quality.

Naive comparison would simply compare local images at different parts of material surface. The Figure 13 depicts image samples of the same woven material at two different locations. Image resolution and conditions of acquisition were the same, yet the two images are not equivalent in their spatial properties.

Image subtraction, that takes absolute difference between pair of images, pixel by pixel, yields that images in the Figure 13 are very different. Refer to Figure 14 to see image Figure 13a subtracted from Figure 13b. If the two images were equal, their subtraction would yield zero matrix. It is not true for Figure 14. Any spatial template matching techniques, like image correlation would indicate that presented two images are different. From pixel wise point of view, the answer is yes, images are different. What the answer would be if one compares regularity, repeating shapes and orientation of shapes?

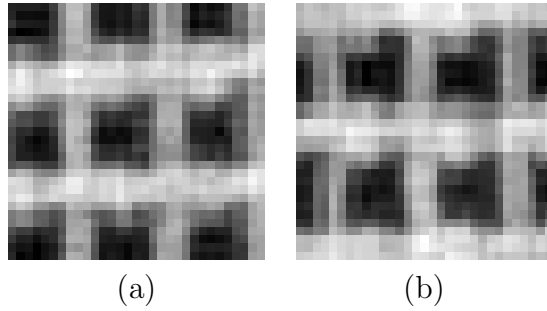


Figure 13: Two sub-images were randomly selected from large image of one fabric. Even though this is the same fabric, images definitely do not look the same. Cross correlation, subtraction or convolution, any spatial template matching methodology would indicate the material in each sub-image as different from another.

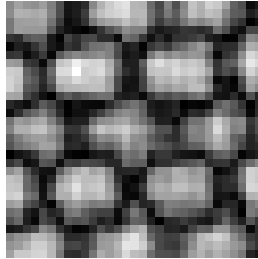


Figure 14: This is absolute difference between image (a) and (b) of Figure 13 presented also as image. The difference is pixel-wise; taking each pixel of (a) subtracting it with corresponding pixel of (b). The result is stored to same location - forming the image as original size. The bright pixels indicate great difference between (a), (b).

The approach to inspect whether weft and warp yarns, in the two images in Figure 13, interrelate equally, does not consist in measuring absolute positions of objects (yarns). More useful and less misleading would be taking into account periodicity at given orientation of yarns. For that purpose, each filter from set of Gabor filters is applied power spectrum of image Figure 13a,b. Instead of computing inverse of filtered spectrum, as has been shown in previous section, one takes mean μ and standard deviation σ of power spectrum coefficients weighted with each filter. Assuming the sub image is of resolution $N \times N$ and a bank consist of M filters, the listed steps are followed:

1. Multiply Figure 13a with 2D Hamming window. Results in $N \times N$ image.
2. Compute 2D Discrete Fourier Transform (DFT) of windowed spatial image. Results in $N \times N$ power spectrum.

3. Multiply frequency plane with single filter from bank of Gabor filters. Results in $N \times N$ spectrum (weighted).
4. Compute mean μ and standard deviation σ of all weighted spectrum coefficients. From $N \times N$ matrix to 2×1 vector.
5. Perform previous step for every i -th filter and concatenate each resulting 2×1 vector to form single vector of size $2M \times 1$.
6. Repeat steps 1 through 5 for Figure 13b.

Let the $2M \times 1$ vector be called texture descriptor $\mathbf{r} = (\mu_0, \sigma_0, \mu_1, \sigma_1, \dots, \mu_M, \sigma_M)^T$. Graph in the Figure 15 shows three descriptors. Descriptors a , and b belong to images in Figure 13. The descriptor c belongs to image in Figure 9. All three descriptors were obtained with identical bank of 24 Gabor filters. The two descriptors of texture a and b have similar values. So similar are features of material captured in images. The third descriptor, c , has seemingly different elements from a and b . By means of texture descriptor, \mathbf{r} , similarity between textures might be defined as distance between two descriptors in M dimensional space, R^M .

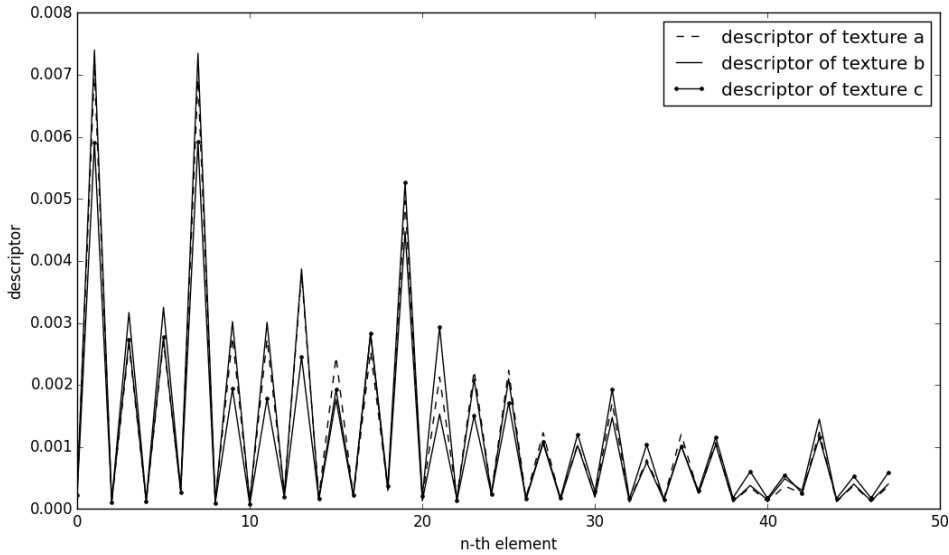


Figure 15: Elements of texture descriptor. The a, b belong to the same material. The descriptor c belongs to different material. The distance between a and b is small which does not apply for distance from a to c , nor the distance from b to c . The descriptor is able to separate textures of different material.

Moving back to task of finding defects in material, the measure of texture sim-

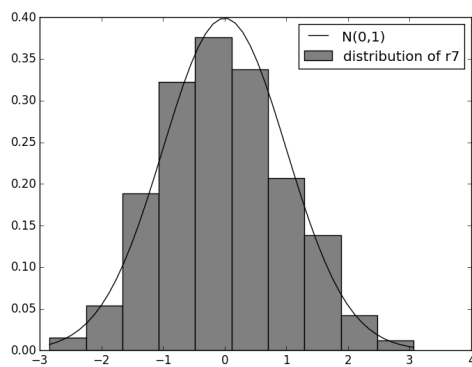
ilarity can be helpful for apparent reason. Visible defects of woven structures introduce level of irregularity on which the descriptor, \mathbf{r} , has proven to be amply sensitive.

Even though, the two images of Figure 13 capture the same structure, certain degree of variability between texture descriptor elements remain. Reasons for that might resist in random noise introduced by camera and/or uneven illumination. Majority of information got lost in the step of reducing $N \times N$ image matrix to $M \times 1$ vector. But the root cause of difference lies in material and weaving process variability, which is inherent and acceptable. We can refer back to Figure 14 and emphasize, that one would hardly find two sub images in large area of woven textile, that would be identical and comparable by means of trivial computer vision techniques.

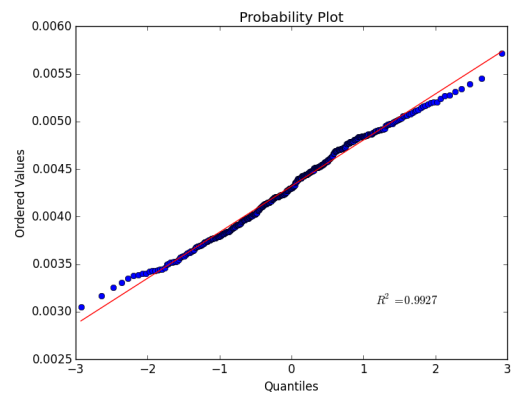
It has been shown up until now, that detection of flaws in textile material is based on comparison between defect free texture and texture containing defect. Evidence has proven that image subtraction or correlation are not suitable for texture content description. Gabor filter has been explained and method to describe texture has been used to evaluate similarity between textures. Low similarity at two different parts of material can indicate defect on one of these places. Still, when two images capture the same pattern in its distinct parts, the descriptor may vary to certain degree. The question is how to find a value that would indicate whether the dissimilarity is governed by natural variation or whether it indicates serious defect.

4.4 Getting to know defect free texture

It has been identified that each element of texture descriptor slightly vary as multiple sub images of defect free texture are captured. The Figure 16a shows histogram of r_7 , the seventh element of texture descriptor \mathbf{r} . Data for the histogram has been taken from 411 sub-images of texture and has been normalized to obey $\mu_{r_7} = 0, \sigma_{r_7} = 1$. The figure also plots PDF of normalized Normal distribution. The Figure 16a is related to previous Figure 15; the histogram in the Figure 16a depicts distribution of single point of Figure 15. While there has been only three sub-images inspected in the Figure 15 and it shows all elements of each descriptor, the histogram in Figure 16a studies distribution of only one, the seventh, element of descriptors taken from set of 411 sub-images. The probability plot, Figure 16b, shows that distribution of r_7 element is in good compliance with Normal distribution. The same applies, and similar plots were generated for the rest of texture descriptor elements. Element seven has been put into figures for illustration here and has no special meaning.



(a)



(b)

Figure 16: Distribution of seventh element of texture descriptor for defect free sample. It happens that if descriptor of defect free texture is computed in many places of texture, then descriptor elements can be considered as normally distributed random variable. Bank of filters consist of 30 Gabor kernels, which produce \mathbf{r} of 60 elements. The histogram is show in figure (a) for seventh element of \mathbf{r} . Other elements are normally distributed as well. The figure (b) shows probability plot with instances of seventh element against normalized normal distribution. Total number of 411 instances have been observed on both figures; all of which come from defect free woven material, see Figure 13 as two such samples.

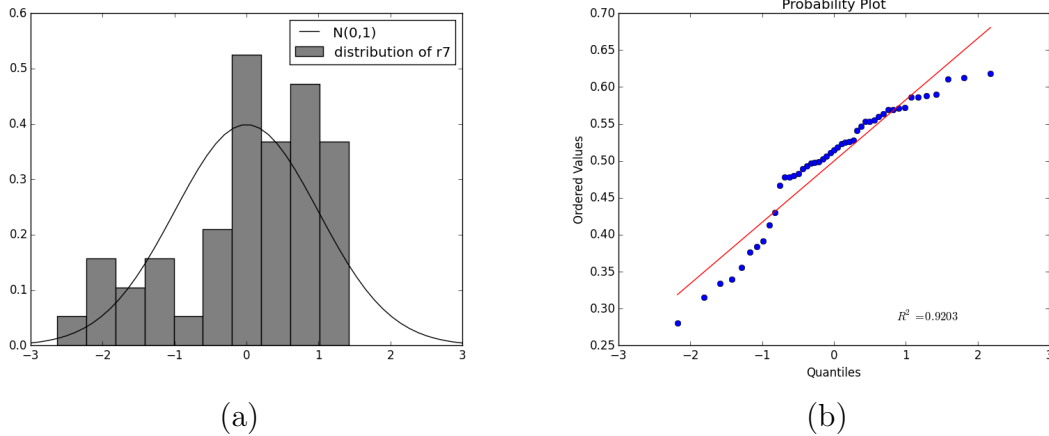


Figure 17: Distribution of seventh element of texture descriptor for positive sample. In contrast to inherent variability of defect free texture, the histogram (a) proofs that elements of descriptor \mathbf{r} , measured with defective material, do not obey Normal distribution. Figure (b) depicts probability plot of 30 samples (normalized) against Normal distribution.

In contrast to normally distributed elements of \mathbf{r} in non-defective samples, the data obtained from images of defects do not exhibit properties of normally distributed data. Histogram and probability plot are depicted in Figure 17.

4.5 Detection of defect

Finding of defect in surface of material can be achieved by distinguishing between descriptor of fine material, \mathbf{r}_n and descriptor of defective material, \mathbf{r}_p . What needs to be defined is listed below.

- Define descriptor of fine material.
- Measure difference between two descriptors.
- Set amount of difference that would indicate a defect.

Definition of fine texture (image of defect free material) is done by means of supervised machine learning. Once image of material is acquired, the image gets annotated by person, who indicates which areas are free of defects and which are not. The Figure 19 shows sample of material that contains defect of broken weft yarn together with annotation that indicates defective area. Detection is done in sub images. Therefore, annotation is discretized into tiles of the same size. Due to

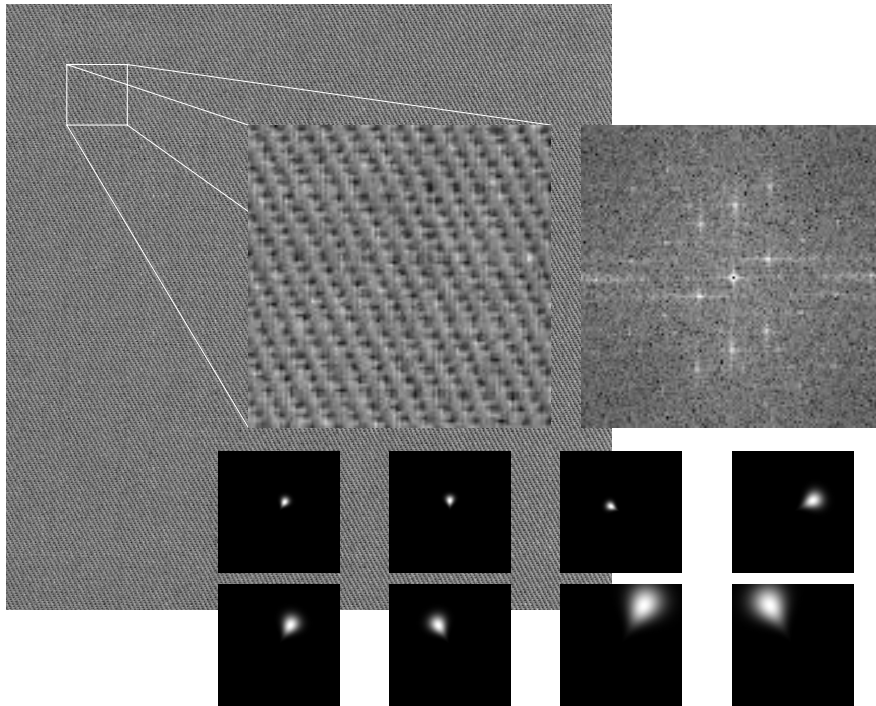


Figure 18: Illustration of textile flaw detection utilizing Gabor filters in frequency domain. Large image of fabric is acquired with two line scan cameras. The large image is sectioned into overlapping sub-images (white rectangle). Each sub-image is transformed to Fourier power spectrum, which then gets weighted by set of Gabor filters.

windowing function, the edges of each sub image are attenuated. The rectangles are generated to overlap by half of width and height not to discard texture on their borders. No detection is performed in this stage. The images is annotated manually for purpose of getting to know the descriptor of defect free material.

As the sample image is annotated, the sub images can be split into two classes. The first class would contain negative samples - images that do not show defect. The second class of positive samples would contain images that contain defect. The set of positive samples consists of red squares in the Figure 19c. For each negative sample, the descriptor \mathbf{r}_n is computed. All descriptors are stacked to form a matrix of negative samples \mathbf{N} , such that each descriptor makes single row of the matrix \mathbf{N} . There are 81 total samples, 74 of which are negative and 7 positive. The bank of Gabor filters contains 30 filters, each producing two elements of \mathbf{r} . The matrix \mathbf{N} has 74 rows and 60 columns. A matrix built up from positive samples, \mathbf{P} , consists of descriptors computed on images containing defect. Hence the matrix \mathbf{P} is of size 7×60 . Now the idea is that descriptors of negative samples, \mathbf{r}_n , the

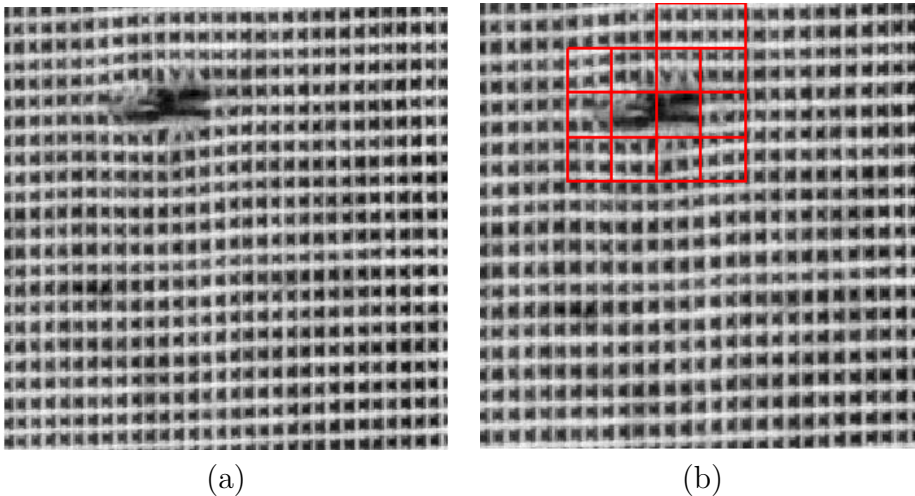


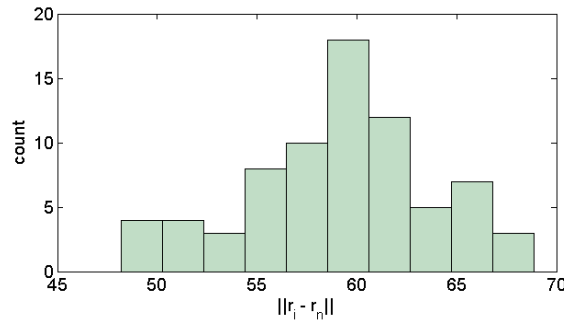
Figure 19: Sample of woven textile containing defect of broken weft yarn. The two line scan cameras capture very large image, but only a portion is displayed in (a). The figure (b) shows annotation of a defect, defined by hand. The annotation is then discretized into tiles of sub image size. The red squares indicate areas of texture that has been annotated as being affected with defect. In order to cover whole image, sub images are generated as overlapping by half of width and height.

vectors in R^{60} are close to each other, while distance between any of \mathbf{r}_n and \mathbf{r}_p , the descriptor of positive sample, would be larger. For the reason that the scale of elements of \mathbf{r} differ, the Mahalanobis distance is computed here. The Mahalanobis distance accounts for and normalizes out the range of elements of vector, by means of covariance matrix. The matrix \mathbf{S} , in equation 14, is the covariance matrix of negative samples matrix \mathbf{N} . Vectors \mathbf{u} and \mathbf{v} are any two rows of \mathbf{N} . The quantity s is distance between the two vectors. The distance s inhere is considered as a reciprocal measure of similarity between two textures, captured by two images in distinct places of material.

$$s = (\mathbf{u} - \mathbf{v})\mathbf{S}^{-1}(\mathbf{u} - \mathbf{v})^T \quad (14)$$

The descriptor of negative samples is defined as expected vector given by mean of each column of \mathbf{N} - the matrix of negative descriptors. Expected descriptor is representation of defect free material. Therefore, the learning stage is complete by:

- Taking \mathbf{r}_n as mean vector from all negative sample descriptors.
- Computing covariance matrix \mathbf{S} from matrix of all negative samples \mathbf{N} .



(a)

	1
1	502.9824
2	1.6043e+03
3	2.7776e+04
4	6.0014e+03
5	1.1436e+03
6	7.4862e+03
7	2.0247e+03

(b)

Figure 20: Distance between negative samples and texture descriptor \mathbf{r}_n is shown as histogram (a). Range of values is between (0,70). Mahalanobis distance, s , between seven positive samples and texture descriptor \mathbf{r}_n is shown here in table (b).

The histogram on the left of Figure 20 shows distribution of Mahalanobis distance between mean negative sample \mathbf{r}_n , and all negative sample descriptors. The table on the right lists equivalent measure between \mathbf{r}_n and the seven positive samples. Because the two ranges do not overlap, there is good chance to split samples into two classes.

Distance, or dissimilarity, is a scalar value. Classification is accomplished by thresholding this quantity. Suitable threshold is estimated by means of Hotelling control statistics. In the process of quality control, the descriptor \mathbf{r} is considered as subject of multivariate statistical process control. The threshold value is given by equation (15), where m , p denote number of observations taken during the phase of learning defect free texture, and the length of descriptor \mathbf{r} , respectively. The value of F represents $(1 - \alpha)$ quantile of Fischer distribution. The upper control limit (UCL) needs to be estimated during learning phase for each texture.

$$UCL = \frac{p(m+1)(m-1)}{m(m-p)} F_{p, m-p}(1-\alpha) \quad (15)$$

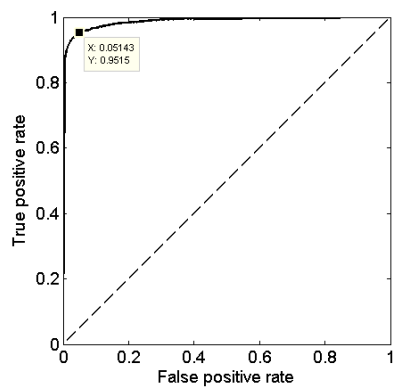
There are 74 samples in present example, the number of sub images. Each sample consists of 60 elements, double the number of filters applied to each sub image. The upper control limit is 704.86 for significance level $\alpha = 0.05$. From data present in Figure 20, all negative samples fall under the upper control limit (*true negative*). Six out of seven positive samples fall above UCL (*true positives*). There is one positive sample that was classified as negative (*false negative*). Results are shown in confusion matrix 1 below .

		Classifier	
		P	N
Truth	P	6	0
	N	1	74

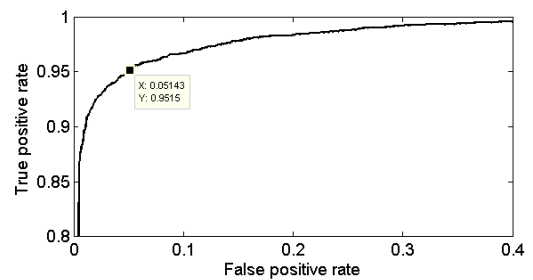
Table 1: Classifier performance with confusion matrix. There is total of 81 samples, 7 of them annotated as positive (contain defect). The classifier miss-classified 1 positive sample as negative, leading to accuracy of 98.7%.

Example above has been given for illustration, and it suffers with insufficient samples, both negative and positive. Annotation has also been made for larger image of equivalent fabric, that contains 6922 negative and 3687 positive samples. The defect has been of broken weft yarn, similar to the defect shown in Figure 19. Having more annotated data, for which the ground truth is known in prior, allows for fine evaluation and tuning of classifier performance. The two performance measures are True positive and False negative rates. The True positive rate, TPR , is a fraction of *true positives* over total number of positive samples. The False positive rate, FPR , reflects number of negative samples classified as positive over total number of negative samples.

Classifier performance can be adjusted by setting the UCL lower toward shorter dissimilarity, resulting in increase of False positive rate - the higher amount of false alarms. By setting the threshold to greater dissimilarities, on the other hand, leads in less false alarms for cost of higher probability of missing detection of true defect. The parameter α of equation 15 has been adjusted between values from 0.001 to 0.1 with step of 0.001. The UCL has been computed for each α and samples had been classified, resulting in TPR and FPR for each threshold. Every TPR has then been plot against corresponding FPR to draw Receiver Operating Characteristic curve. The ROC , shown in the Figure 21, indicates that classifier based on Gabor filters has good ability to separate defects from woven textile. The figure shows two curves actually. The dashed line would represent hypothetic situation in which $\frac{TPR}{FPR} = 0.5$. Corresponding classifier would be equivalent to random guessing. Algorithm would be providing poor detection. The upper left triangle above the diagonal line is space in which any curve indicates better classification. The solid line plots the ROC curve of proposed algorithm. By moving the point toward less amount of False positive rate, one decreases sensitivity of detector and the contrary applies. Selected point of ROC curve is linked to particular UCL during generation of ROC curve and can not be read from the curve alone. It depends on particular needs which point to select and tune the classifier accordingly.



(a)



(b)

Figure 21: ROC curve of algorithm to detect visible defects in fabric. Although two plots are shown, they both display the same curve, but in different resolutions. The figure (a) shows full axes range (0-1). Dashed line indicates random guessing while solid line is performance characteristic of current algorithm. The figure (b) shows the ROC curve in greater detail. Both figures indicate single point on the curve, which means the *UCL* for which the algorithm indicates 95.15% of true defects and it produces false alarm in 5.14% of sub-images. Data for the measurement come from material shown in the Figure 19.

5 Experiment

Selected fabric defects has been tested during experiments. Detection of defects has been performed with methodology explained in section 4. Representative experiments are shown below.

The device captures at resolution of about 10 pixels per millimeter. The size of sliding window depends on type of fabric. The smaller the window, the smoother detection can be achieved. On the other hand, the size of sub-image needs to be so large to capture repeating pattern of fabric, including discarded edges that get attenuated with Hamming window. Generally the size of square sliding window has been 64 pixels.

Testing set has been selected to contain defects in direction of weft, defects in way of warp and defects of fabric that have no directional dependence. Images of fabric are gray. The nature of detection is to recognize visible defects in structure, not variance in color of material.

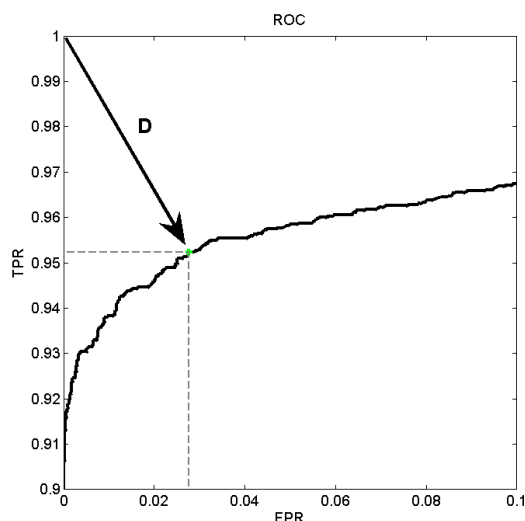


Figure 22: Setup of particular classifier is achieved by seeking point on ROC curve, that's distance to coordinate (0,1) is minimal. The solid curve indicates performance for different upper control limits, see equation 15. By using higher UCL, the detection would indicate less false positives but also less true positives. Decreasing UCL would lead to the opposite. There is no the one correct setup, since it depends on required performance. Using the point, that is closest to top-left corner of the graph, the combination of TPR, FPR is closest to perfect classifier. Note: axis limits are (0;0.1) on FPR axis and (0.9;1) on TPR axis.

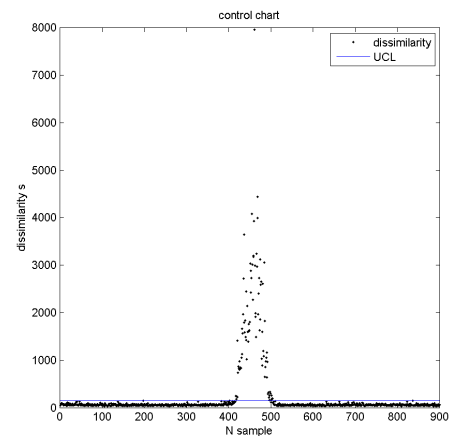
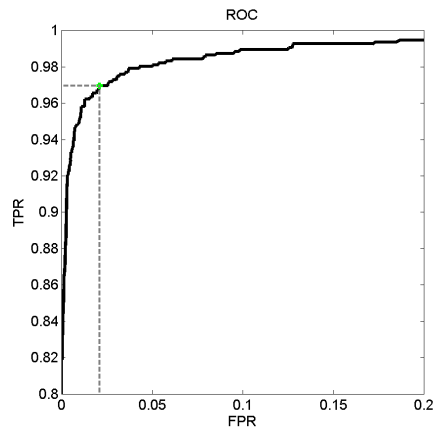
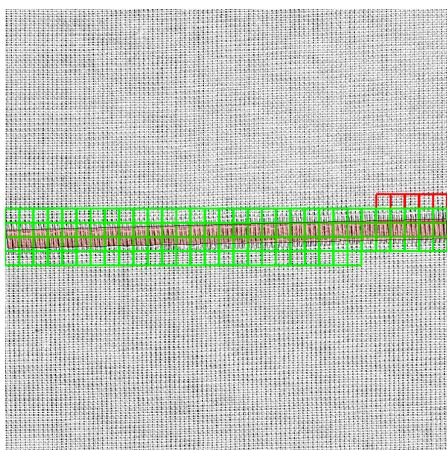
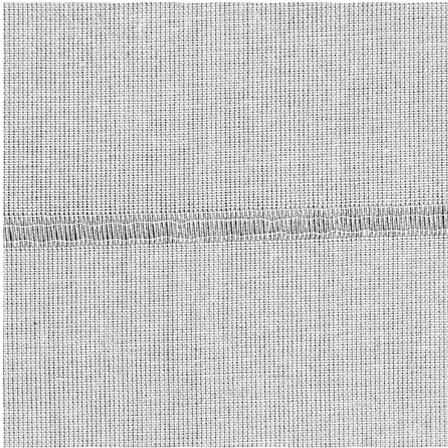
Experiment has been conducted as follows. First the material has been annotated by supervisor. Annotation splits the whole image into area which contains the defect (positive samples) and area which is of desired quality (negative samples). Negative samples have been taken from portion of defect-free area, which represented a training set. Training samples have been used to learn descriptor of a texture together with covariance matrix of texture descriptor elements. Previous steps represent supervised learning stage of the algorithm. After the learning stage, the algorithm has been applied on rest of data - the entire surface, excluding the training set.

Results are displayed with four figures; the top left figure shows plain image of fabric. Performance of detection is expressed with ROC curve in top right figure. All graphs highlight single point on ROC curve, which is the point of ROC curve, closest to the upper left corner of the graph. The upper left corner represents the performance of perfect classifier with no false positive and 100 % true positive rate. The vector D stands for distance vector in Figure 22. The bottom left figure displays green and red squares over the image of fabric. The red squares indicate false positives, while the green squares indicate true positives. The red polygon indicates annotation of defect. The bottom right figure shows Hotelling control chart with blue line meaning the upper control limit and black dots that show dissimilarity between descriptor of good material and descriptor of current sub-image. Sub-images (squares) have been generated systematically from left to right, top to bottom. Sub-images overlap here by one half of width and height.

5.1 Thin place

Description of defect

Insufficient density of weft threads. Visible as strip that usually extends across the full width of the fabric. Can be a symptom of beat-up mechanism malfunction.



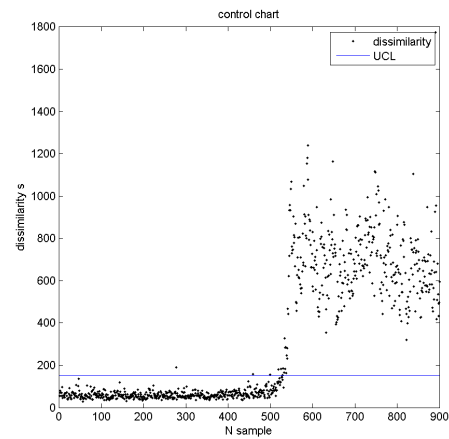
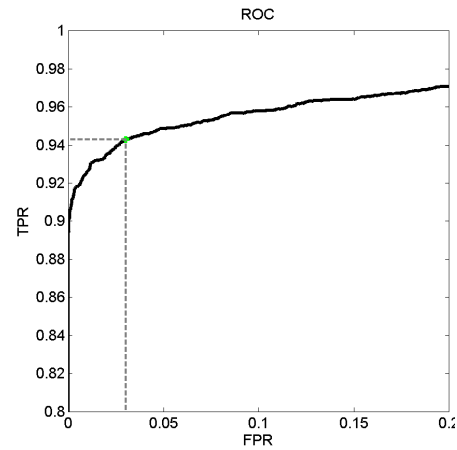
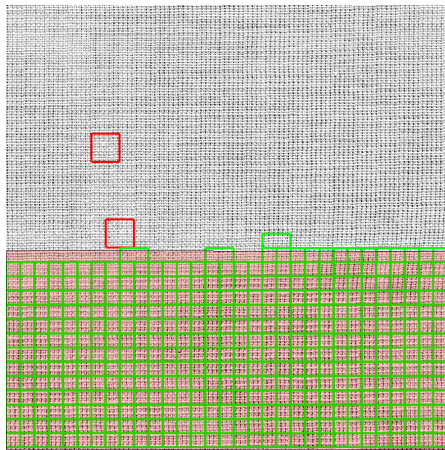
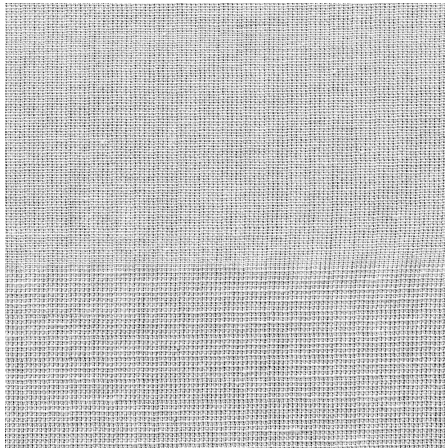
Comment on algorithm performance

Total of six false positives are present in this example. It is obvious, from control chart in bottom-right, that UCL has been set unnecessarily low. Hence the presence of false positives. Even if UCL was doubled, the algorithm would indicate much of true positives and none of false positives. The dissimilarity is large enough for much of positive samples to be detected safely.

5.2 Irregular weft density

Description of defect

Systematic change in density of weft yarns that spans across whole width of fabric and occupies large area.



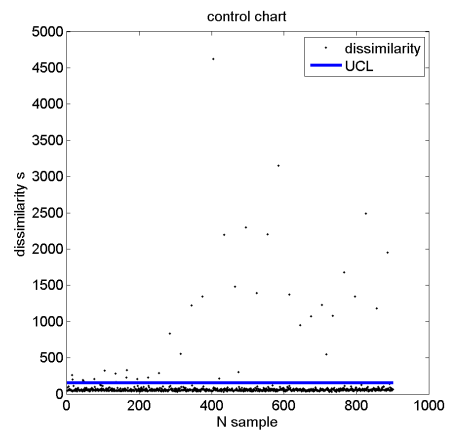
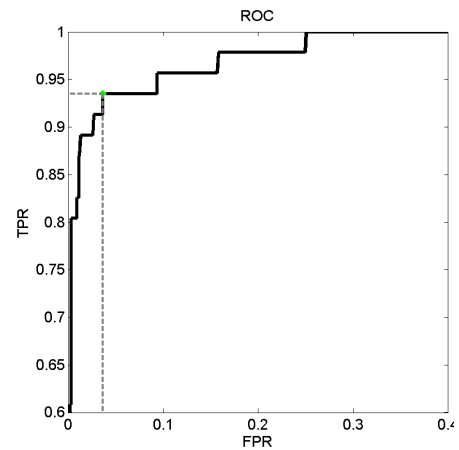
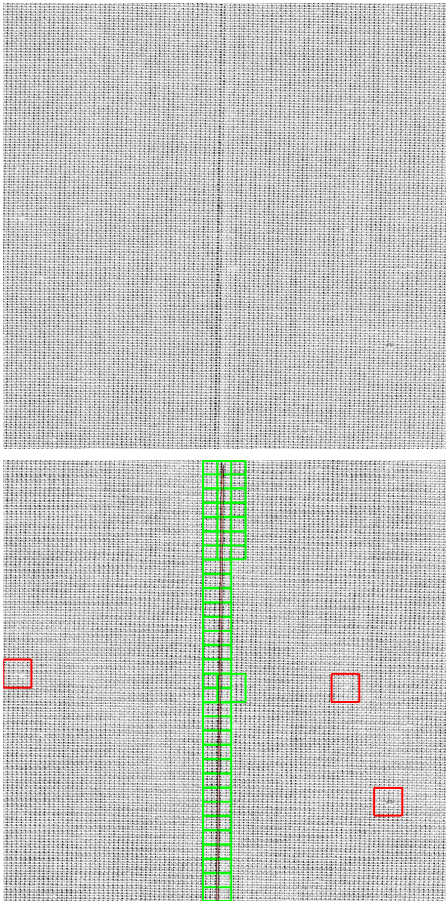
Comment on algorithm performance

Incorrect density of weft yarns at the bottom of the image, appears as brightness that is different from rest of fabric. Performance of classification is 94% of true positive rate and 3% false negative rate as indicated by dashed lines and a point on ROC curve. Different performance can be achieved, either to prefer lower false positives or increase true positives.

5.3 Broken warp yarn

Description of defect

Single or more warp yarns missing. Visible as insufficient warp density, a stripe of certain length.



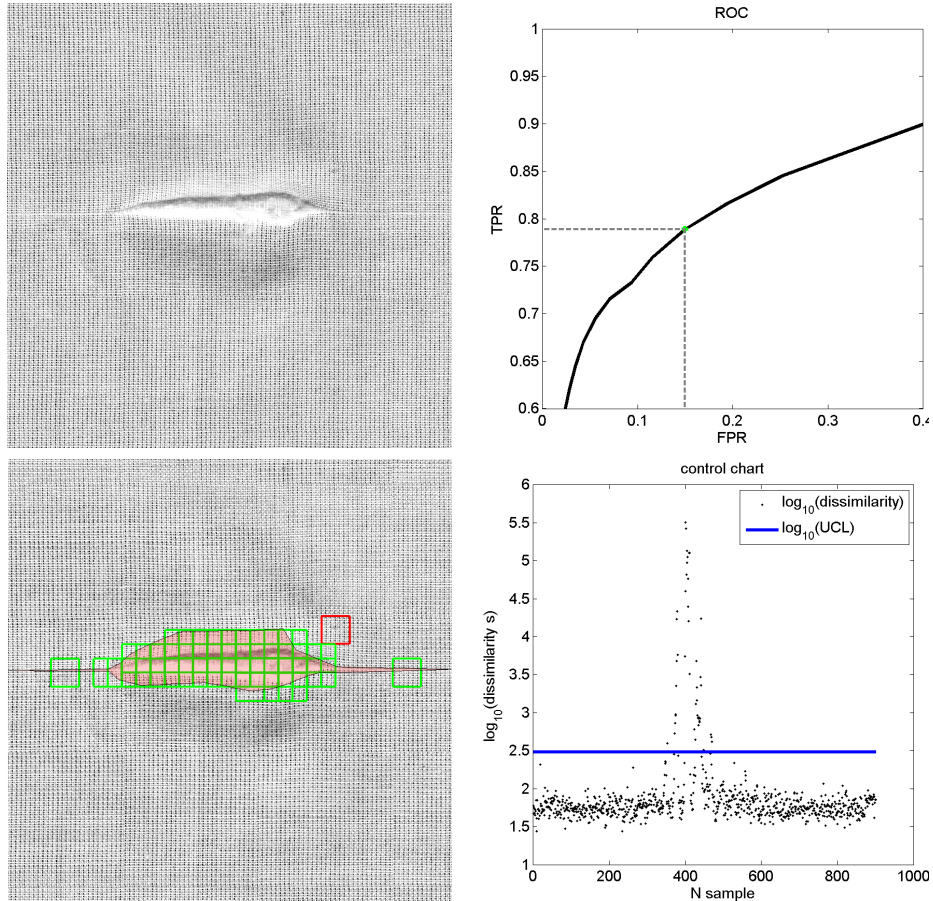
Comment on algorithm performance

Appears as thin strip in vertical direction. Interlacing of threads is not correct. Density of warp yarns is also wrong. The ROC curve is not as smooth as in other experiments due to lower number of available samples.

5.4 Yarn defect

Description of defect

Thick yarn, visible as abrupt change in fabric; distorts neighboring yarns.



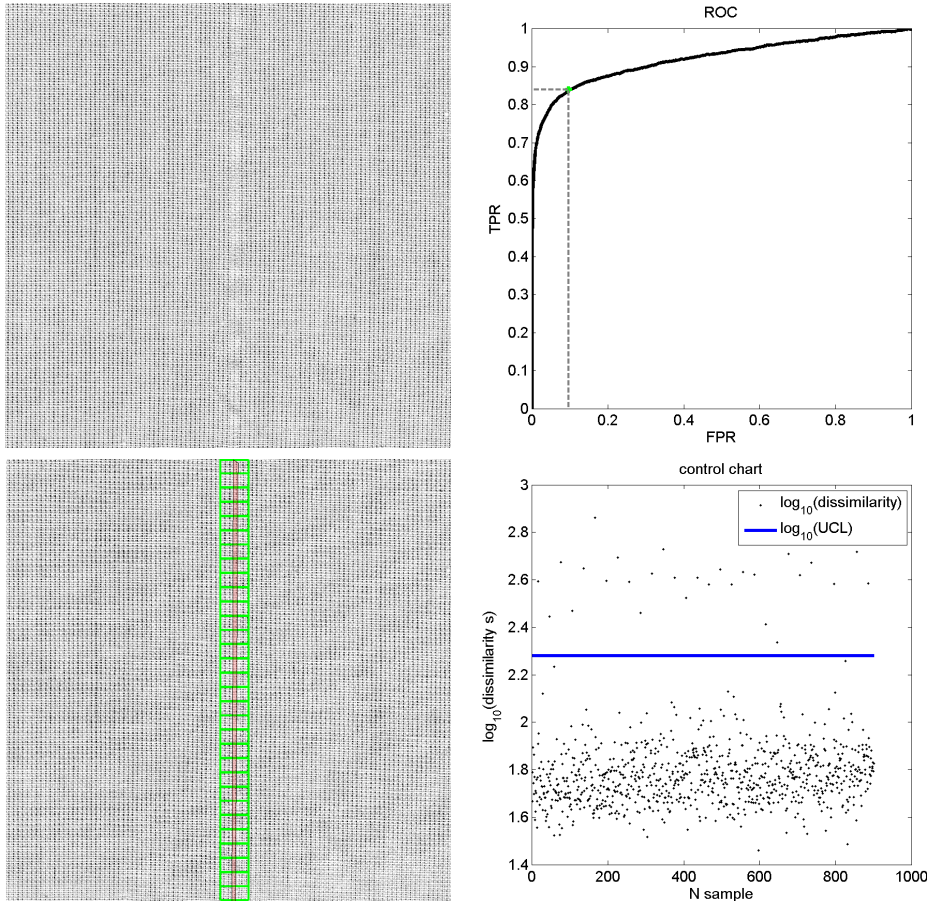
Comment on algorithm performance

Defect can be detected with high confidence, as the descriptor changes extensively. The defect affects neighboring yarns and makes it difficult to draw sharp border between positive and negative area (the annotation). Hence ROC curve does not indicate very good classification. On the other hand, the change in texture descriptor is so large that the control chart vertical axis had to be drawn in logarithmic scale to display values reasonably.

5.5 Harness misdraw

Description of defect

Two yarns drawn wrong. Vertical stripe all along the fabric.



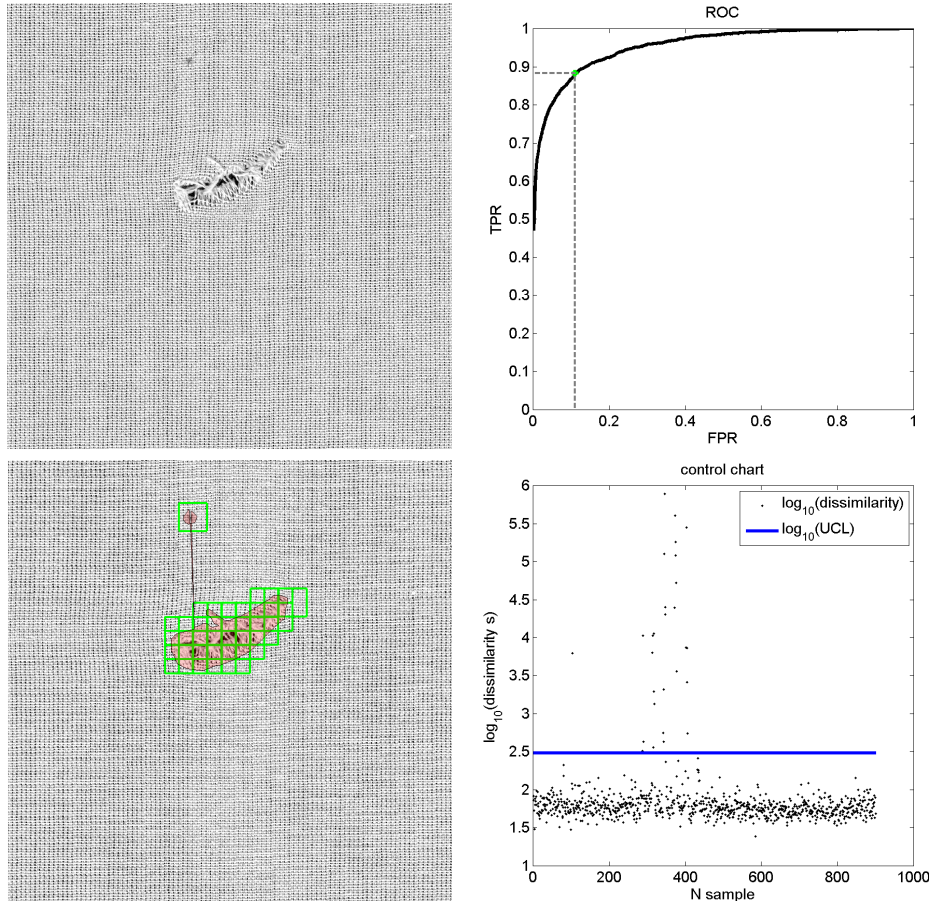
Comment on algorithm performance

Logarithmic scale has been used for plotting control chart as well for harness misdraw defect.

5.6 Hole

Description of defect

Group of broken weft or warp yarns. Well detected as local deviation of brightness. As tension of broken yarns is different, the neighboring yarns get misaligned, too.



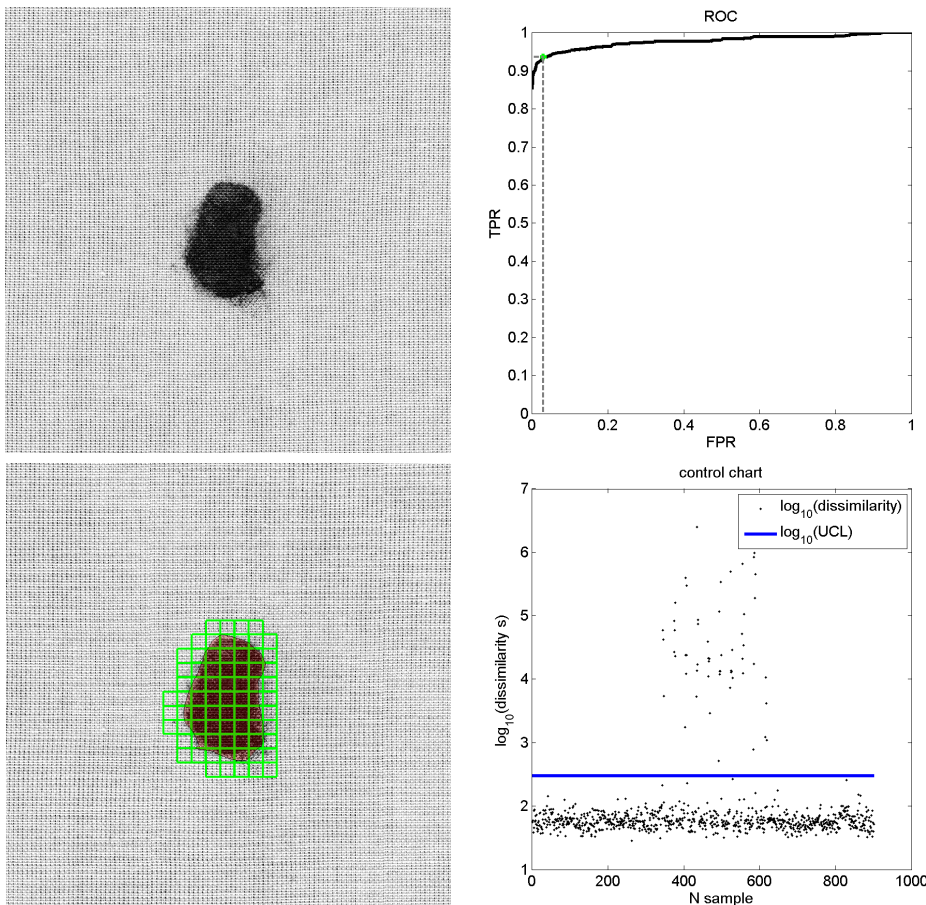
Comment on algorithm performance

There are actually two holes in the image. Larger one is obviously visible in the center of the image. The second, smaller, defect is in upper part of the image. Refer to the annotation drawn with the red polygon.

5.7 Stain

Description of defect

Oil soiling causes local change in color, easily distinguishable. Causes no distortion in structure of material from periodicity and orientation point of view.



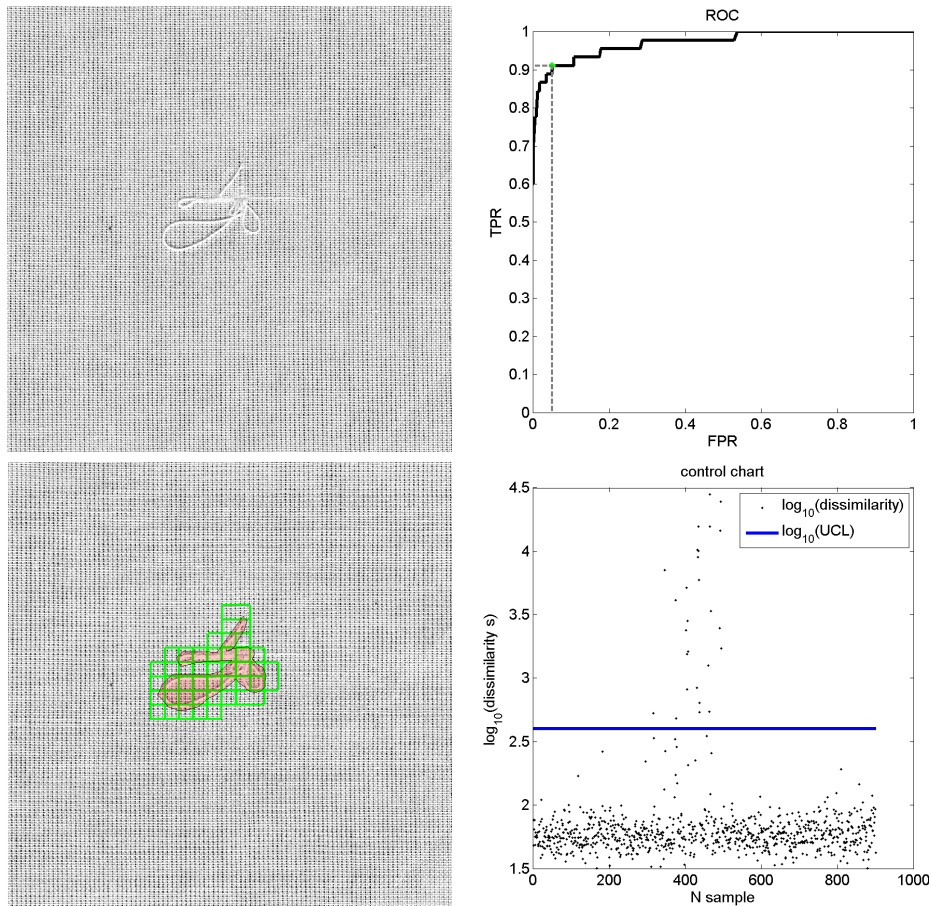
Comment on algorithm performance

The algorithm performs the best for this type of defect. It would be well detected with simpler method than proposed algorithm. Important feature is that only filters that operate at low frequencies influence texture descriptor and have effect on algorithm performance. Filters at middle and high frequencies could possibly be skipped without decreasing performance of detector.

5.8 Snag

Description of defect

Single or group of yarns dragged from alignment. Yarns of less density can cause visible stripe along the fabric.



Comment on algorithm performance

Strong edges in orientations different from regular fabric: Strong response is granted.

The measurement of classifier performance depends on how well the defect gets annotated. For certain cases, it might be difficult to draw a sharp border around a defect. If the annotation is wrong, then certain number of sum-images fall into wrong category; truly positive annotated as negative and vice versa. Under such circumstances, distorted texture descriptor is estimated in learning stage. The

second problem is that whole image is discretized into sub-images. The problem considers how the sub-image is placed relative to the defect. If the rectangular sub-image hits the annotated area (belongs to true positive) but only portion of defect is contained in the sub-image but the rest is of regular fabric, it is likely that algorithm is going to decide badly and produce false negative. Then, higher number of miss classifications happen during the inspection stage, which results in increased false positive rate and decreased true positive rate. This applies for any kind of defect. But, in practical application, it is satisfactory when only one sub-image indicates a defect.

6 Conclusion

The thesis deals with the design and implementation of visual inspection device in context of textile structures. The purpose of the device is to perform detection of apparent defect of fabric. Among topics described in the thesis belong the concept and assembly of the device, the architecture of component based software, and specific image processing techniques that enable the inspection of a textile structure. Special attention is put to the aspect of inspection device, which seems to be a neglected issue in existing publications. The problem is inherent to any visual inspection device and is associated with the acquisition of digital image itself. The thesis points out that the placement of cameras at the inspection device and relative position of cameras is in fact the cause of deformations of objects in the image of line scan camera. The deformation prevents the images of two adjacent cameras to be simply put side by side without any corrections made to the images. Comprehensive study has been given on the projection characteristics of a line scan camera, which has led to creation of an entirely unique method of image rectification. Thanks to the method, developed in the section 3, it is possible to eliminate image distortion and merge images of an array of line cameras into the overall scene. This is important in context of textiles, in which the surface of material reaches several meters in width and acquisition with multiple cameras is natural solution. The idea of projecting the image of real camera to the image of an ideal camera, given in the section 3, is the key feature of the thesis. From the perspective of the author, the findings obtained in the section dedicated to image acquisition represent the most important contribution of the thesis to the current stage of knowledge in the field visual monitoring of textiles.

The second part of the thesis is dedicated to the method of spectral analysis of the image of textiles, which is based on filtering the frequency spectrum of the image of fabric. The fundamental principle of the method is based on the experience that planar textiles consist of regularly interconnected system of yarns which give the image of such structure a unique visual properties. Complex structure, such as a fabric, can be effectively expressed in the frequency space. It is shown and explained in the thesis how the frequency spectrum of the image of the fabric elegantly captures the repeating structure using small number of parameters. It has been found that a presence of a defect negatively affects the spectrum of regular structure in a way that provides an opportunity to detect the presence of the defect. For that reasons the proposed method of detection of defects describes the planar textiles and implements the detection of defects using the spectral analysis approach given in the section 4. The detection of defect is specified as a problem of assessing the similarity of local texture given the descriptor of the correct texture. As the tool for assessing the similarity between two textures,

a set of Gabor filters has been applied to the spectra of each texture. With respect to the requirement to run the inspection in real time, the frequency analysis has been implemented using the latest software design methods, which include task parallelism, asynchronous data processing and calculations offloaded from the main processor to the the graphics accelerator. Thanks to the applied methods of software design, it has been possible to run the inspection algorithm on-line over real data, in real conditions, on custom designed inspection device; all of which has proved the functionality of both the proposed algorithm, and the entire system. The system, mainly from software point of view, has not been designed and assembled solely for the purpose of this work. In fact the opposite is true. The inspection device states for completely open system in which the proposed inspection algorithm is only one of many elements, which can be supported, or completely replaced by another visual inspection method.

In relation to the defects of fabrics, the thesis neither aim to explanation of their impact on quality of final textile product, nor does it address the original cause of defects. This topic is beyond the scope of this work, which deliberately provides brief description of each defect in the section of experiments. The thesis concentrates on the classification performance of the proposed algorithm.

Despite convincing inspection performance, the weak part of the algorithm is the bank of filters itself. The filters are generated statically. No respect is given to the visual features of particular defect. For that reason, it may happen that certain filters of the bank have little effect on the classification. It may also happen, on the other hand, that the important part of the frequency spectrum, which is crucial for the discovery of the defect, is not covered with any particular filter. The danger of missing the defect occurs when the important part of the spectrum is located on the border between two filters. Both filters carry the spectrum with the coefficient of one half, thus attenuating the important feature. Certainly the static bank of Gabor filters is not the optimal solution. The state of the art techniques of image segmentation and texture classification are methods based on the deep neural networks. These are methods of supervised learning, in which a man builds arbitrary hierarchy of linear operations which are applied to the input signal. The advantage of neural networks is the training step, during which the network learns the optimal coefficients of operation itself, given the training data. It is the computational power of graphics cards and availability of computer clusters that can handle excessive number of computations required during iterative deep learning of current complex networks. With respect to material inspection of textiles, especially the convolutional neural networks, that include hidden layers, seem to be capable of learning the optimal filters themselves, given samples of fabric and the defect [42].

7 References

- [1] A Kumar. “Computer-Vision-Based Fabric Defect Detection: A Survey”. In: *Industrial Electronics, IEEE Transactions on* 55.1 (2008), pp. 348–363. ISSN: 0278-0046. DOI: 10.1109/TIE.1930.896476.
- [2] A Kumar and G.K.-H. Pang. “Defect detection in textured materials using Gabor filters”. In: *Industry Applications, IEEE Transactions on* 38.2 (2002), pp. 425–440. ISSN: 0093-9994. DOI: 10.1109/28.993164.
- [3] Yong M. R. Ro et al. “MPEG-7 Homogeneous Texture Descriptor”. English. In: *ETRI Journal* 23.2 (2001), pp. 41–51.
- [4] Mishra Loonkar Shweta and Dharendra. “A Survey-Defect Detection and Classification for Fabric Texture Defects in Textile Industry”. English. In: *International Journal of Computer Science and Information Security* 13.5 (May 2015), pp. 48–56.
- [5] Yi G. Shu and Li X. Tang. “Automated Visual Inspection for Medicines in Aluminum-Plastic Blister Packaging”. English. In: *Applied Mechanics and Materials* 325-326 (June 2013). pp,38-40, p. 1267.
- [6] Jože Derganc et al. “Real-time automated visual inspection of color tablets in pharmaceutical blisters”. In: *Real-Time Imaging* 9.2 (2003), pp. 113–124. ISSN: 1077-2014. DOI: [http://dx.doi.org/10.1016/S1077-2014\(03\)00018-4](http://dx.doi.org/10.1016/S1077-2014(03)00018-4).
- [7] N. S. S. Mar, P. K. D. V. Yarlagadda, and C. Fookes. “Design and development of automatic visual inspection system for PCB manufacturing”. English. In: *Robotics and Computer Integrated Manufacturing* 27.5 (2011), pp. 949–962.
- [8] Mohit Borthakur, Anagha Latne, and Pooja Kulkarni. “A Comparative Study of Automated PCB Defect Detection Algorithms and to Propose an Optimal Approach to Improve the Technique”. English. In: *International Journal of Computer Applications* 114.6 (2015). Copyright - Copyright Foundation of Computer Science 2015; Last updated - 2015-04-18.
- [9] J. Kula, M. Tunak, and A. Linka. “Tvorba vzorovaných tapet pomoci rovinnych grup symetrie (Creating patterned ditranslational design by group of symmetry)”. In: *Moderní matematické metody v inženýrství (3μ)*. 2010. ISBN: 978-80-248-2342-3.

- [10] Henry Y.T. Ngan, Grantham K.H. Pang, and Nelson H.C. Yung. “Motif-based defect detection for patterned fabric”. In: *Pattern Recognition* 41.6 (2008), pp. 1878–1894. ISSN: 0031-3203. DOI: <http://dx.doi.org/10.1016/j.patcog.2007.11.014>. URL: <http://www.sciencedirect.com/science/article/pii/S003132030700502X>.
- [11] Maroš Tunák et al. “Estimation of fiber system orientation for nonwoven and nanofibrous layers: local approach based on image analysis”. In: *Textile Research Journal* 84.9 (2014), pp. 989–1006.
- [12] Manuel Ferreira, Cristina Santos, and Joao Monteiro. “A texture segmentation prototype for industrial inspection applications based on fuzzy grammar”. English. In: *Sensor Review* 29.2 (2009), pp. 163–173.
- [13] Jianli Liu, Baoqi Zuo, and Xianyi Zeng. “The visual quality recognition of nonwovens using a novel wavelet based contourlet transform”. English. In: *Multimedia Tools and Applications* 70.3 (June 2014). Copyright - Springer Science+Business Media New York 2014; Last updated - 2014-08-31, pp. 1667–1684.
- [14] Ding-Kuo Huang and Chi-Feng Chen. “Supervised learning method and quality capability of process used in an optical transmission inspection of on-line nonwoven basis weight”. In: *Optics Communications* 285.8 (2012), pp. 2106–2112. ISSN: 0030-4018. DOI: <http://dx.doi.org/10.1016/j.optcom.2011.12.008>. URL: <http://www.sciencedirect.com/science/article/pii/S0030401811013708>.
- [15] Wayne C. Tincher, Wayne Daley, and Wiley Holcomb. “Detection and Removal of Fabric Defects in Apparel Production”. English. In: *International Journal of Clothing Science and Technology* 4.2 (1992). Copyright - Copyright MCB University Press Limited 1992; Last updated - 2014-05-23; CODEN - ICSTEH; SubjectsTermNotLitGenreText - US, p. 54.
- [16] L. Norton-Wayne, M. Bradshaw, and A. J. Jewell. “BMVC92: Proceedings of the British Machine Vision Conference, organised by the British Machine Vision Association 22–24 September 1992 Leeds”. In: ed. by David Hogg and Roger Boyle. London: Springer London, 1992. Chap. Machine Vision Inspection of Web Textile Fabric, pp. 217–226. ISBN: 978-1-4471-3201-1. DOI: [10.1007/978-1-4471-3201-1_23](http://dx.doi.org/10.1007/978-1-4471-3201-1_23). URL: http://dx.doi.org/10.1007/978-1-4471-3201-1_23.
- [17] Yixiang Frank Zhang and Randall R. Bresee. “Fabric Defect Detection and Classification Using Image Analysis”. In: *Textile Research Journal* 65.1 (1995), pp. 1–9. DOI: [10.1177/004051759506500101](http://dx.doi.org/10.1177/004051759506500101). eprint: <http://trj.sagepub.com/content/65/1/1.full.pdf+html>. URL: <http://trj.sagepub.com/content/65/1/1.abstract>.

- [18] A.S. Tolba and A.N. Abu-Rezeq. “A self-organizing feature map for automated visual inspection of textile products”. In: *Computers in Industry* 32.3 (1997), pp. 319–333. ISSN: 0166-3615. DOI: [http://dx.doi.org/10.1016/S0166-3615\(96\)00076-0](http://dx.doi.org/10.1016/S0166-3615(96)00076-0). URL: <http://www.sciencedirect.com/science/article/pii/S0166361596000760>.
- [19] A. C. Bovik, M. Clark, and W. S. Geisler. “Multichannel texture analysis using localized spatial filters”. In: *IEEE Transactions on Pattern Analysis and Machine Intelligence* 12.1 (1990), pp. 55–73. ISSN: 0162-8828. DOI: 10.1109/34.41384.
- [20] Jarle Strand and Torfinn Taxt. “Local frequency features for texture classification”. In: *Pattern Recognition* 27.10 (1994), pp. 1397–1406. ISSN: 0031-3203. DOI: [http://dx.doi.org/10.1016/0031-3203\(94\)90072-8](http://dx.doi.org/10.1016/0031-3203(94)90072-8). URL: <http://www.sciencedirect.com/science/article/pii/0031320394900728>.
- [21] Phil Brodatz. *Textures : a photographic album for artists and designers*. New York: Dover Publications, 1966. ISBN: 0-486-21669-1. URL: <http://opac.inria.fr/record=b1084586>.
- [22] R. M. Haralick, K. Shanmugam, and I. Dinstein. “Textural Features for Image Classification”. In: *IEEE Transactions on Systems, Man, and Cybernetics* SMC-3.6 (1973), pp. 610–621. ISSN: 0018-9472. DOI: 10.1109/TSMC.1973.4309314.
- [23] T. P. Weldon and W. E. Higgins. “Design of multiple Gabor filters for texture segmentation”. In: *Acoustics, Speech, and Signal Processing, 1996. ICASSP-96. Conference Proceedings., 1996 IEEE International Conference on*. Vol. 4. 1996, 2243–2246 vol. 4. DOI: 10.1109/ICASSP.1996.545868.
- [24] T. P. Weldon and W. E. Higgins. “Integrated approach to texture segmentation using multiple Gabor filters”. In: *Image Processing, 1996. Proceedings., International Conference on*. Vol. 3. 1996, 955–958 vol.3. DOI: 10.1109/ICIP.1996.560980.
- [25] A. Teuner, O. Pichler, and B. J. Hosticka. “Unsupervised texture segmentation of images using tuned matched Gabor filters”. In: *IEEE Transactions on Image Processing* 4.6 (1995), pp. 863–870. ISSN: 1057-7149. DOI: 10.1109/83.388091.
- [26] D. Dunn and W. E. Higgins. “Optimal Gabor filters for texture segmentation”. In: *IEEE Transactions on Image Processing* 4.7 (1995), pp. 947–964. ISSN: 1057-7149. DOI: 10.1109/83.392336.

- [27] D. Dunn, W. E. Higgins, and J. Wakeley. “Texture segmentation using 2-D Gabor elementary functions”. In: *IEEE Transactions on Pattern Analysis and Machine Intelligence* 16.2 (1994), pp. 130–149. ISSN: 0162-8828. DOI: 10.1109/34.273736.
- [28] T. Randen and J. H. Husoy. “Filtering for texture classification: a comparative study”. In: *IEEE Transactions on Pattern Analysis and Machine Intelligence* 21.4 (1999), pp. 291–310. ISSN: 0162-8828. DOI: 10.1109/34.761261.
- [29] A. Bodnarova, M. Bennamoun, and S. Latham. “Optimal Gabor filters for textile flaw detection”. In: *Pattern Recognition* 35.12 (2002). *Pattern Recognition in Information Systems*, pp. 2973–2991. ISSN: 0031-3203. DOI: [http://dx.doi.org/10.1016/S0031-3203\(02\)00017-1](http://dx.doi.org/10.1016/S0031-3203(02)00017-1). URL: <http://www.sciencedirect.com/science/article/pii/S0031320302000171>.
- [30] A. Kumar and G. K. H. Pang. “Defect detection in textured materials using Gabor filters”. English. In: *IEEE Transactions on Industry Applications* 38.2 (2002), pp. 425–440.
- [31] R. Han and L. Zhang. “Fabric Defect Detection Method Based on Gabor Filter Mask”. In: *2009 WRI Global Congress on Intelligent Systems*. Vol. 3. 2009, pp. 184–188. DOI: 10.1109/GCIS.2009.356.
- [32] Alper Baykut et al. “Real-time Defect Inspection of Textured Surfaces”. In: *Real-Time Imaging* 6.1 (2000), pp. 17–27. ISSN: 1077-2014. DOI: <http://dx.doi.org/10.1006/rtim.1998.0153>. URL: <http://www.sciencedirect.com/science/article/pii/S107720149890153X>.
- [33] K. L. Mak and P. Peng. “An automated inspection system for textile fabrics based on Gabor filters”. English. In: *Robotics and Computer Integrated Manufacturing* 24.3 (2008), pp. 359–369.
- [34] Yao Sun and Hai ru Long. “Adaptive detection of weft-knitted fabric defects based on machine vision system”. In: *The Journal of The Textile Institute* 102.10 (2011), pp. 823–836. DOI: 10.1080/00405000.2010.523192. eprint: <http://www.tandfonline.com/doi/pdf/10.1080/00405000.2010.523192>. URL: <http://www.tandfonline.com/doi/abs/10.1080/00405000.2010.523192>.
- [35] M. Tunák, A. Linka, and P. Volf. “Load-sharing and Monte Carlo models of defects in a bundle of fibres”. In: *Composites Science and Technology* 69.9 (2009). Special Issue on the 12th European Conference on Composite Materials (ECCM12), organized by the European Society for Composite Materials (ESCM), pp. 1417–1421. ISSN: 0266-3538. DOI: <http://dx.doi.org/10.1016/j.compscitech.2008.09.004>. URL: <http://www.sciencedirect.com/science/article/pii/S0266353808003400>.

- [36] Maroš Tunák, Aleš Linka, and Petr Volf. “Automatic assessing and monitoring of weaving density”. In: *Fibers and Polymers* 10.6 (2010), pp. 830–836. ISSN: 1875-0052. DOI: 10.1007/s12221-009-0830-1. URL: <http://dx.doi.org/10.1007/s12221-009-0830-1>.
- [37] Maros Tunák and Ales Linka. “Directional Defects in Fabrics”. English. In: *Research Journal of Textile and Apparel* 12.2 (May 2008). pp. 539 - 549, pp. 13–22.
- [38] “Analysis of Planar Anisotropy of Fibre Systems by Using 2D Fourier Transform, journal =”. In: ().
- [39] Maros Tunak et al. “Estimation of fiber system orientation for nonwoven and nanofibrous layers: local approach based on image analysis”. English. In: *Textile Research Journal* 84.9 (June 2014), pp. 989–1006.
- [40] Tunak Maros, Bajzik Vladimir, and Testik M. Caner. “Monitoring chenille yarn defects using image processing with control charts”. English. In: *Textile Research Journal* 81.13 (Aug. 2011), pp. 1344–1353.
- [41] Francesco Bianconi and Antonio Fernández. “Evaluation of the effects of Gabor filter parameters on texture classification”. In: *Pattern Recognition* 40.12 (2007), pp. 3325 –3335. ISSN: 0031-3203. DOI: <http://dx.doi.org/10.1016/j.patcog.2007.04.023>. URL: <http://www.sciencedirect.com/science/article/pii/S003132030700218X>.
- [42] Jiuxiang Gu et al. “Recent Advances in Convolutional Neural Networks”. English. In: (2015).

8 Author’s publications

- [1] Lucie Vysloužilová et al. “Needleless coaxial electrospinning: A novel approach to mass production of coaxial nanofibers”. In: *International Journal of Pharmaceutics* 516.1–2 (2017), pp. 293 –300. ISSN: 0378-5173. DOI: <http://dx.doi.org/10.1016/j.ijpharm.2016.11.034>. URL: <http://www.sciencedirect.com/science/article/pii/S0378517316310869>.
- [2] J. Kula et al. “Image analysis of jet structure on electrospinning from free liquid surface”. In: *Applied Physics Letters* 104.24, 243114 (2014), pp. –. DOI: <http://dx.doi.org/10.1063/1.4884597>. URL: <http://scitation.aip.org/content/aip/journal/apl/104/24/10.1063/1.4884597>.
- [3] M. Tunák et al. “Estimation of fiber system orientation for nonwoven and nanofibrous layers: local approach based on image analysis”. In: *Textile Research Journal* 84.9 (2014), pp. 989–1006.

- [4] M. Tunak, J. Kula, and J. Chvojka. “Estimation of Fibre Systems Orientation”. In: *Information Bulletin*. Vol. 4. Czech Statistical Society, 2012, pp. 265–271. DOI: <http://dx.doi.org/10.5300/IB>.
- [5] J. Kula. “Automation of a Standard Test Method for Grading Spun Yarns for Appearance”. In: *Structure and Structural Mechanics of Textiles*. 2012.
- [6] J. Kula, M. Tunak, and A. Linka. “Inspection system of fabric based on texture segmentation utilizing Gabor filters”. In: *The 2011 International Conference on Data Engineering and Internet Technology*. Bali, Indonesia, 2011.
- [7] J. Kula, M. Tunak, and A. Linka. “A Fibrous Object Segmentation by Predominant Orientation”. In: *18th International Conference STRUTEX*. Technical University of Liberec. 2011, pp. 87–93.
- [8] J. Kula, M. Tunak, and A. Linka. “Real-time defect detection of fabrics”. In: *The International Symposium on Stochastic Models in Reliability Engineering, Life Sciences and Operations Management*. Beer Sheva, Izrael, 2010.
- [9] J. Kula, M. Tunak, and A. Linka. “Tvorba vzorovaných tapet pomocí rovinových grup symetrie (Creating patterned ditranslational design by group of symmetry)”. In: *Moderní matematické metody v inženýrství (3μ)*. 2010. ISBN: 978-80-248-2342-3.
- [10] J. Kula et al., eds. *Reliability, Quality and Estimation 2009 (REQUEST'09)*. Proceedings editor. Technical University of Liberec. Nov. 2009.
- [11] J. Kula, M. Tunak, and Linka. *Zařízení pro vizuální monitorování kvality textilních struktur, prototyp*. 2009.
- [12] J. Kula et al. “Studium hladinového elektrostatického zvlákňování (Analysis of Needle-less Electrospinning From Free Surface of Liquid)”. In: *Technical Computing Prague 2008*. Humusoft s.r.o., 2008.

9 Published papers

Title: Image Analysis of Jet Structure on Electrospinning from Free Liquid Surface

Abstract The work analyses intra-jet distances during electrospinning from a free surface of water based poly(vinyl alcohol) solution confined by two thin metallic plates employed as a spinning electrode. A unique computer vision system and digital image processing were designed in order to track position of every polymer jet. Here, we show that jet position data are in good compliance with theoretically predicted intra-jet distances by linear stability analysis. Jet density is a critical parameter of electrospinning technology, since it determines the process efficiency and homogeneity of produced nanofibrous layer. Achievements made in this research could be used as essential approach to study jetting from two-dimensional spinning electrodes, or as fundamentals for further development of control system related to NanospiderTM technology.

Journal: Applied Physics Letters

Impact factor: 3.739

Submission: L14-00090R2

Editor: Orlando Auciello

Title: Estimation of fiber system orientation for nonwoven and nanofibrous layers: local approach based on image analysis

Abstract Analysis of textile materials often includes measurement of structural anisotropy or directional orientation of textile object systems. To that purpose, the real-world objects are replaced by their images, which are analyzed, and the results of this analysis are used for decisions about the product(s). Study of the image data allows one to understand the image contents and to perform quantitative and qualitative description of objects of interest. This paper deals in particular with the problem of estimating the main orientation of fiber systems. Firstly, we present a concise survey of the methods suitable for estimating orientation of fiber systems stemming from the image analysis. The methods we consider are based on the two-dimensional discrete Fourier transform combined with the method of moments. Secondly, we suggest abandoning the currently used global, that is, all-at-once, analysis of the whole image, which typically leads to just one estimate of the characteristic of interest, and advise replacing it with a local analysis. This means splitting the image into many small, non-overlapping pieces, and estimating the characteristic of interest for each piece separately and independently of the others. As a result we obtain many estimates of the characteristic of interest, one for each sub-window of the original image, and - instead of averaging them to get just one value - we suggest analyzing the distribution of the estimates obtained for the respective sub-images. The proposed approach seems especially appealing when analyzing nonwoven textiles and nanofibrous layers, which may often exhibit quite a large anisotropy of the characteristic of interest.

Journal: Textile Research Journal

Impact factor: 1.135

10 Unpublished papers

Title: Practical implementation of inspection system using Gabor filters

Abstract This paper deals with both hardware and software setup of a system dedicated for on-line control of visual quality parameters of fabric. The device is based on aluminium frame, parallel line scan digital cameras and traction mechanism. Related software implementation has been developed as a modular system of independent components, that provide tools like image acquisition, motion control, stitching of images and image analysis. Certain implementation of Gabor filter for description of texture and subsequent texture segmentation has been described. The filters are applied in a new method of defect detection of dissimilarities of fabric during it's quality inspection process. Design of Gabor filter is presented both in spatial and frequency domain. Description of planar texture has been treated as a vector of responses of the texture to given bank of filters. Ratio of similarity between two different textures is proposed and also applied in the process of detection of defects. Proposed method has been implemented as a software components and it has been tested, together with dedicated inspection device, to proof it's real-time performance.

Journal: Elsevier - Expert System with Applications

Impact factor: 1.965

Submission: ESWA-D-11-01587

Editor: Jay Liebowitz

Response: Thank you for sending your above paper for possible publication in ESWA. Although it was felt that your research was quite interesting, we are publishing only the most highly rated papers for publication in ESWA in order to maintain our high rankings and impact factor. Those papers that aren't selected typically could improve in a number of areas such as a more thorough discussion of the design, development, testing and evaluation results; clarifying the key significance of the research contribution; making sure the references are the most recent in your paper's research field of relevance; ascertaining that the research fits the aims and scope of the journal; and a better command and flow of English writing throughout the paper. We are very sorry for this inconvenience, but appreciate your interest in the journal. Regards. Jay Liebowitz, Editor

Title: Needleless coaxial electrospinning: a novel approach to mass production of coaxial nanofibers

Abstract Herein, we describe a novel, simple spinneret setup for needleless coaxial electrospinning that exceeds the limited production capacity of current approaches. This approach also leads to the formation of coaxial nanofibers with a higher and uniform shell/core ratio, which results in the possibility of better tuning of the degradation rate. These parameters favor the broader application of coaxial nanofibers from weir spinnerets as systems for controlled drug delivery in regenerative medicine and tissue engineering.

Journal: Nano Letters

Impact factor: 12.940

Submission: nl-2012-03701z

Curriculum Vitae

Personal Data

Place and Date of Birth: Czech Republic — 5. August 1983
Address: Lhotska 2204, Prague, 193 00, Czech Republic
Phone: +420 736 773 399
Email: jiri.kula@hotmail.com

Education

Jul 2012 | Bachelor of Computer Science
Czech Technical University in Prague, Faculty of Electrical Engineering
Department of Computer Graphics and Interaction
Thesis: 'Calibration of multi-camera system'
Advisor: Daniel Sykora, Ph.D

Jul 2008 | Master of Textile Engineering
Technical University of Liberec, Faculty of Textile Engineering
Department of Nonwoven Textiles
Thesis: 'Analysis of Needleless Electrospinning From Free Surface of Liquid'
Advisor: prof. David Lukas

Languages

English | *TOEFL iBT*® score: 101 out of 120

Czech | Mother tongue

Work Experience

<i>Current</i> Dec 2014	Vision research engineer <i>Valeo Research & Development, Prague, Czech Republic</i> Design of computer vision algorithms for automotive industry. Integration into embedded hardware.
Oct 2014 Mar 2013	Developer for Nikon imaging software <i>Laboratory Imaging Ltd., Prague, Czech Republic</i> Software development in hardware division of NIS-Elements microscope imaging software. Responsible for integration of number of different devices for advanced microscopy and image processing, including Illumination/Stimulation laser devices, Digital cameras, Motorized microscope stages.
Jan 2013 Sep 2010	Research assistant <i>Technical University of Liberec</i> Worked as a research assistant at Department of Textile Evaluation. Led seminars in subjects of Numerical mathematics, Root finding methods and Basics of image processing using Matlab.
Jan 2012 Sep 2011	Multiple Camera Calibration <i>Czech Technical University in Prague</i> Solved the task to calibrate omnidirectional device made out of six wide angle cameras in order to achieve spherical panorama from all cameras. The principle is featured in commercial products known as <i>Camera Ball</i> .
<i>Current</i> Sep 2008	Automatic visual control system for textile structures <i>Technical University of Liberec</i> Development of machine consisting of multiple line scan cameras capturing image of surface of fabric in order to reveal visible defects during production process. Emphasized on componentized software architecture and integration within diverse range of applications. Development of innovative method of texture description. Solved within dissertation thesis. <i>Planned end date: fall 2014.</i>
Jun 2008 Sep 2007	Object tracking during production of nano fibers <i>Technical University of Liberec</i> Tracking of polymer solution behavior under the action of high voltage. Observation and estimation of nano fiber production contributed to development of principles that Nanospider™ technology is based on. Solved within diploma thesis.
Apr 2008 Aug 2006	C# developer <i>Baud Ltd., Prague, Czech Republic</i> Member of a team to contribute in development of client and database application for leading Czech estate agency. Specialization on XSLT, XML, Web-Services, plug-in development on Microsoft .NET Framework.

Grants received

Dec 2012	Device to measure the amount of fibres protruding from structure of a yarn
Feb 2012	ARM and Linux based embedded device for image acquisition and image processing. Supported by The Ministry of Education, Youth and Sports of the Czech Republic (Student's grant competition TUL in specific University research in 2012), project No. 4868. Project leader — Amount of grant: 133, 100 CZK (6, 000 USD) — Project duration: 1 year
Dec 2011	Research Center for Quality and Reliability of Production
Jan 2008	Development of a methodology for quality improvement, diagnostics and reliability analysis of production and technological processes, namely with respect to their applicability in practice. The advancement of complex analytic methods, leading to increase of competitiveness of industrial works. Project co-worker — Amount of grant: 70, 772, 000 CZK (3, 078, 000 USD) — Total project duration: 6 years
Dec 2011	Fiber segmentation from image of textile structure using orientation property
Feb 2011	Application of Gabor spatial filter to estimate physical properties of nano fibers from their image. Supported by The Ministry of Education, Youth and Sports of the Czech Republic (Student's grant competition TUL in specific University research in 2011), project No. 4830. Project leader — Amount of grant: 130, 000 CZK (6, 000 USD) — Project duration: 1 year
Dec 2010	Implementation of methods for on-line quality control of textile structures
Feb 2010	Research on spatial filters suitable for texture classification. Supported by The Ministry of Education, Youth and Sports of the Czech Republic (Student's grant competition TUL in specific University research in 2011), project No. 4823. Project leader — Amount of grant: 332, 800 CZK (9, 500 USD) — Project duration: 1 year
Dec 2009	Automatic visual defects detection of textile structures
Feb 2009	Internal student's grant competition at Technical University of Liberec. Team of three under graduate students were involved as co-researchers. Project no. IGS-FT-TUL 136/2009 Project leader — Amount of grant: 211, 000 CZK (15, 000 USD) — Project duration: 1 year

Courses taught

Jan 2013		Image Processing
Sep 2009		Introduction to numerical analysis Methods of Stochastic and Simulating Methods (As member of the Department of Textile Evaluation at Technical University of Liberec)

Theses supervised

Jan 2011		Segmentation of fibrous objects in digital picture on the basis of their directional
Sep 2010		orientation
Sep 2010		The impact of used filter and the type of filtration on the purity of milk
Jan 2011		
Sep 2009		Detection of Defects of Woven Fabric Using Gabor Filters
Jan 2010		

ZÁPIS O VYKONÁNÍ STÁTNÍ DOKTORSKÉ ZKOUŠKY (SDZ)

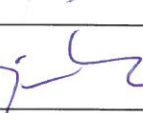
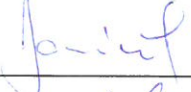
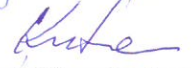
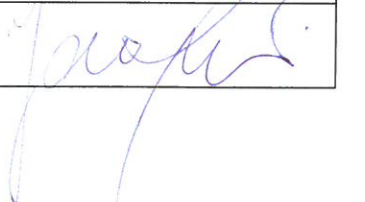
Jméno a příjmení doktoranda: **Ing. Jiří Kula**
Datum narození: **5. 8. 1983**
Doktorský studijní program: **Textilní inženýrství**
Studijní obor: **Textilní technika**
Termín konání SDZ: **3. 12. 2014**

 **prospěl**

 **neprospěl**

Komise pro SDZ:

Podpis

Předseda:	prof. Ing. Jiří Militký, CSc.	
Místopředseda:	prof. RNDr. Jan Píček, CSc.	
Členové:	doc. Ing. Vladimír Bajzík, Ph.D.	
	doc. RNDr. Miroslav Brzezina, CSc.	
	RNDr. Dr. Jiří Janáček	
	doc. Ing. Antonín Kuta, CSc.	
	prof. Ing. Jaroslav Šesták, DrSc., dr.h.c.	

V Liberci dne 3. 12. 2014

O průběhu SDZ je veden protokol.



V Liberci, dne 2. 11. 2016

Disertační práce:
AUTOMATIC VISUAL CONTROL SYSTEM FOR TEXTILE PROCESSES

Autor: Ing. Jiří Kula

Hodnocení recenzenta

Disertační práce Ing. Jiřího Kuly „AUTOMATIC VISUAL CONTROL SYSTEM FOR TEXTILE PROCESSES“ se zabývá konstrukcí a softwarem zařízení pro automatickou průběžnou kontrolu hodnocení kvality tkanin na základě snímání jejich vizuálních parametrů. Doktorand vyvinul modulární programové vybavení z nezávislých komponent, které poskytují následující funkce: snímání obrazu, řízení pohybu, skládání obrazů a obrazovou analýzu. Pro segmentaci textury a její identifikaci byly použity tak zvané Gaborovy filtry. Tyto filtry jsou použity jak v prostorové, tak ve frekvenční oblasti analýzy obrazu. Gaborovy filtry jsou využity jako originální metoda detekce defektů tkanin. Doktorand navrhl poměr podobnosti mezi dvěma různými texturami, který použil pro detekci vad. Krom tohoto základního tématu se doktorand zabýval také obrazovou analýzou procesu stejnosměrného elektrického zvlákňování.

Jiří Kula zahájil svoji doktorskou práci pod školitelem prof. RNDr. Alešem Linkou, CSc. Osobně jsem se stal školitelem až v posledním roce jeho studia po tragické nehodě jmenovaného pana děkana. Jiřího Kulu jsem poznal jako mimořádně nadaného, samostatného, invencí a pracovní pílí překypujícího studenta.

Doktorand ve své práci použil Gaborovy filtry ve frekvenční oblasti pro výpočet odlišností/podobností mezi soubory různých textur. Odhad těchto podobností byl použit pro kontrolu kvality tkaných textilií. Jednalo se přitom zejména o zjištění a lokalizaci vad. Doktorand samostatně navrhl, zkonstruoval a postavil specializovaná laboratorní zařízení za účelem vyhodnotit možnost použití Gaborových filtrů pro kontrolu kvality povrchu textilií v reálných podmínkách. Zkonstruované zařízení je schopné zaznamenat digitální obraz pohybující se tkaniny prostřednictvím několika čtecích kamer. Obraz je dále zpracováván pomocí doktorandem navrženého vysoce výkonného software v reálném čase. Doktorand ukázal, že Gaborovy filtry realizované v jím navrženém a zkonstruovaném hardwarovém i softwarovém prostředí jsou vhodným prostředkem pro kontrolu kvality povrchů textilií v reálném čase. Ke kontrole dochází s dostatečnou přesností pro některé druhy viditelných vad plošných textilií.

Jako zcela dostatečnou hodnotím publikační činnost Ing. Jiřího Kuly, která čítá sedm konferenčních příspěvků ve sbornících a dvě časopisecké publikace. Za vynikající úspěch považuji uveřejnění práce s názvem „Image analysis of jet structure on electrospinning from free liquid surface“, která byla publikována v časopise Applied Physics Letters. Zmíněný časopis se nachází na prestižním seznamu Nature Index.

Práce J. Kuly přispěla k rozvoji aplikace analýzy obrazu pro moderní textilní technologii.

Navrhuji, aby práce Ing. Jiřího Kuly byla přijata k obhajobě.

prof. RNDr. David Lukáš, CSc.



Opponent Report For the PhD's dissertation of Ing. Jiří Kula

Prepared By: *Doc. Ing. Mohamed Eldessouki, PhD*
Technical University of Liberec, Liberec

Date: August 25, 2016

This is an evaluation report for the PhD dissertation submitted by Ing. Jiří Kula (henceforth: "the author") and entitled "Automatic Visual Control System For Textile Processes" at the Technical University of Liberec, Liberec, Czech Republic. This report is a response to the request of the dean of the Faculty of Textiles Ing. Jana Drašarová, Ph.D. (Č.j. TUL-16/4814/027828) and to fulfill the partial requirements of the defense committee chaired by Prof. Ing. Jiří Militký, CSc. (Č.j. TUL-16/4814/005710).

The report is organized in *four* separate sections that start with a description of the dissertation, then a "discussion and evaluation" of its components are given in section 2 where a detailed reasoning is provided for our final recommendations (given in section 4). General comments on the dissertation layout and the use of language are also included in section 3 of this report.

1 Description

I received a printed copy of the dissertation as well as a compacted disk (CD) that contains a digital copy of the dissertation and the source files for the presented work. The dissertation consists of a *front-matter* (that includes: abbreviations, contents, and abstract), and 101 pages that present a *body* of six chapters (introduction, objectives, pinhole and line scan camera models, image processing, experiment, and conclusion), as well as a *back-matter* (four appendices, references, and the author's publications).

The *first* chapter introduced the investigated problem of this research (the manual evaluation of fabric's quality parameters), and some of the methods introduced in the literature to handle this problem based on fabric's image analysis. The author suggested the use of Gabor filters as an effective tool for extracting the textural descriptors of the fabric. This chapter was concluded by presenting the organization of the dissertation.

The *second* chapter highlighted the main procedures of the work, and described the hardware and the software implemented in this dissertation. This hardware section includes figures for the prototype inspection machine, and the software was presented as a modular platform that allows addition/omission of modules without affecting the total performance of the system.

The *third* chapter described the image acquisition model in a pinhole and a line-scan camera with a mathematical description of the image representation and the algorithms for calibrating, correcting and reconstructing panoramic images of the acquired object based on two (or more) cameras.



The *forth* chapter presented the methodology suggested by the author to handle the investigated problem. A description of Gabor filters and their affecting parameters was given, then the algorithm for identifying the textural descriptors and their extraction from the fabric images. This chapter presented also the method for discriminating between defected and defect-free samples, the thresholding technique, and the detection performance based on some quantitative measures.

The *fifth* chapter presented the results of applying the suggested technique with case studies for some common fabric faults and the detection performance in each case.

The dissertation *closes* with a conclusion followed by appendices for matrix decomposition, homogeneous coordinates, windowing algorithm, and software's component interface. The references of the dissertation were given, then a list of the author's publication was provided.

2 Discussion and Evaluation

The topic of this dissertation is very important in the fields of fabric production and its evaluation. The success of achieving an "automatic visual control system for textile processes" should lead to a consistent fabric production that does not depend on the human intervention and makes the process economically efficient. This research topic is still active with many challenges that need to be solved through a continuous research, and the work presented in this dissertation shall be considered in that context. **The following paragraphs** summarize my comments and evaluation on the topics, *in the same order* of their presentation through the thesis.

The *title* of the dissertation has a broad range, especially when it refers to "textile processes". If changing the title is allowed at this stage, it would be preferred to use more specific title that reflects the presented work and its main scope.

The *first chapter* for introduction has a *fragmented structure*, where the ideas are not presented in a *logical* order. For example, the *contribution* of the work is presented at the first page of the chapter, then the *motivation* behind the work was introduced. Similarly, towards the end of the chapter, the author *distinguished* his work from the available literature, *then* introduced more work from the literature. **To fix this problem**, it is recommended to avoid the *long mixed* paragraphs and present each main idea in a *separate* paragraph, then combine these paragraphs to cover a specific element of the work. I recommend this chapter to present the upcoming elements in the following *suggested* order: *definition* of the problem, its *importance* and the *motivations* behind its solution, *available methods* of solution, *shortcomings* of the available methods, *suggested hypothesis* by the author to deal with these shortcomings, *uniqueness* of the suggested approach, and an overview of the suggested *procedures* to test the *validity* of the hypothesis. These elements already exist, *to some extent*, in the current manuscript and the author can use the suggested order to restructure this chapter. It should be clear that, this comment is provided *as an example* in this chapter, and an *analogy* should be utilized for *the other chapters*.





Regarding the used references for this work; while it is important to focus on the *textural methods* and their *performance* in the introduction (as they are more related to the topic of the thesis), the *scope* of coverage should be *wider* to extend for *other methods* and efforts in the field. Also, the majority of references used in the presented survey are *outdated* and do not catch up with the recent advances on the topic. According to these two comments, the author should be very *conservative* in giving *general opinions*, such as saying "No scientific work has been published....". In fact, such statements arise from *mixing the absence of evidence with the evidence of absence*, which is a major *trap* for generalization.

The *second* chapter carries the title of "objectives", which is *misleading* and does not reflect the materials that were presented in the chapter. Hence, a *change* of the chapter's title will be useful. Although the chapter presents a detailed structure of the hardware and software, there was no definitive answer to questions such as: what is the linear speed of the prototype machine (the text only refers to 0.87 m/s as a *camera limit*)? Or, whether the system performs *online* or *offline* analysis? The author argues that *it is both*, but it will be more useful to give a *specific definition* for the analysis type *then* identify the system *according to* this definition. Also, it is not convincing for the reader to *list* some advantages of a line-scan camera, while the presented work *does not utilize* these advantages in the given analysis.

For the *software utilization* in this chapter; The author argues in different places of the thesis that, the main contribution of this *whole work* to the current state of knowledge is the algorithm for *correcting* the captured image and projecting the *actual camera image* to the *ideal camera image*. Regardless of the *accuracy* of this statement and the *existence* of similar calibration and correction methods in the literature, the introduced software structure utilized the CameraLink and the Multiplexor to capture the images and stitch them together to form the final image of analysis. Both of these modules (as well as the other used modules) are standard "filters" of the DirectShow software, and it is not clear how these *standard* algorithms utilize the "*new*" correction algorithm described in Chapter 3? Therefore, it is of a special importance to clearly identify the *actual contributions* by the author to build the analysis software and the parts he *developed* versus the *ready-made* ones.

This question leads to a description for the CD attached with the thesis. There is neither *organization* nor *instruction* on using the files on the CD. Most of the files are not usable, even the simple Matlab script files do not function properly and depend on certain files and commands that are not included. Since the author decided to attach the software part to the thesis, it should be presented in a way suitable for the PhD dissertation. As a general rule, if an item (sentence, paragraph, computer file,...etc.) does not *add* to the work, it will automatically *subtract* from its value. That means, the author should be *more careful* in presenting the work in the written form *as well as* in the accompanied digital form.

Progress of ideas and derivations in chapter *three* is relatively clear to follow. However, the introduction of matrix **A** and **B** after Equation (29) is not obvious whether they refer to the ideal (non-rotated) camera image (i.e. $\mathbf{A} = y_a = U_A X$ and $\mathbf{B} = y_b = U_B X$) or not? Especially that, the symbol **A** was used in a different context with Equation (2).



The idea of "automation" does not have *enough evidence* and *might collapse* based on the given work in *chapter 4* (and in *chapter 5*). For example, to show the effect of Gabor filter on the periodic structure, the author demonstrated the results in Figures 21-23; nevertheless, these figures were produced under *selected* and *optimized* conditions (the same applies to results of *chapter 5*). This means that, a *prior knowledge* about the samples is required for a *proper adjustment* of the values of parameters Θ and Ω that create the set (or the bank) of filters. Also, picking "element No. seven" (which represents the mean μ and standard deviation σ at a specific filter *distance* and *orientation*), as a representative for all texture descriptor is another evidence of this *selectivity* and *bias* regarding the performance of the system with each sample. This *prior knowledge* poses questions about the *credibility* of the "automatic system" and its *validity*, while the author admitting in *chapter 5* that: "...It is never known in advance, which kind of defect is going to appear during production".

Another *major issue* of results in chapters 4 and 5 is the *lack of distinction* between the *detection* and the *classification* processes. Generally, there is only a "defect detection" system in this work and "no classifiers" are presented. The system can be called "classifier" if it has the ability to deal with *multiple fabric faults* under the same condition (i.e. same analysis algorithm with the same settings for Gabor filters), and having the ability to distinguish (i.e. *classify*) each fault type. However, in this work, each fault type was treated with a different set of Gabor filters (with *optimized* and *a priori known parameters*) which allowed it to "detect" the fabric fault, not to "classify" it. For the distinction between *classifiers* and *detectors*, the author might check a previous work by Eldessouki *et al.* in *FIBRES & TEXTILES in Eastern Europe* 2014; 22, 4(106): 51-57.

Related to the previous point: the efficiency of detection for the system is misleading, because it is calculated based on a single defect type. It should be more informative about the system's performance if the efficiency of the same *detector* is measured with samples of different defect types. As a matter of fact, it will be really surprising if the performance of the given *supervised* and *optimized* system is less than 90%. In other words, and just to give *one* example: what will be the performance of detectors in sections 5.3 and 5.5, which have filters with $(\Theta, \Omega) = (24,0)$, $(24,30)$ and $(24,90)$, if they were used in detecting fabric faults of sections 5.1, 5.4, 5.6 and 5.7 which *also* use the same set of filters?

In a similar fashion that demonstrates the *biased* efficiency of the detection systems and how they are *tailored* to specific samples, the author stated in section 5.2 that "Much of what has been described for the thin place defect also applies for irregular weft density". If these defects (5.1 and 5.2) are similar, why only *two* filters were used in the first defect, while *computationally demanding eleven* filters were required in the second case? The same logic applies to faults in sections 5.3 and 5.5 that were described as "similar" because they show "vertical strips along the material". Since both faults are *visually similar*, why using different filter sets in each case? From the analytical point of view, these questions are understandable and can easily be answered; however, these questions are given here to indicate the importance of avoiding the *misguidance* to the readers, and the need to *clarify the facts* while documenting the results.





Regarding the *definitions* and the *categorization* of fabric faults; the "thin places" (in section 5.1) are well known defects in the *spinning* industry (i.e. *yarn* defects), while its use in the thesis refers to *a variation of the weft density* is not accurate. Technologically, this defect occurs due to a stop/start of the weaving machine and that is why it is usually called a "stop-mark". Similarly, it might be more suitable to categorize fabric faults according to the *orientation* of their occurrence in warp, weft, or areal directions (please refer to the above reference for details), especially that Gabor filters are also sensitive to their orientation.

There is a great *ambiguity* about the *samples size* in this work. If I understood it correctly, the total number of points plotted in the results for each fault type represents the number of sub-windows within the detected sample. In other words, it seems like, the whole system is based on a *single image for each type* of fabric faults, and this image is used for calculating the control limits of the system (i.e. its training), as well as its testing and validation. *If this interpretation is true* (as I said, it is really ambiguous), the *credibility* of the suggested system will be *questionable*; because no system can be built and *generalized* based on a *single observation* (regardless of the number of sub-readings obtained *within* that observation).

In section 5.4, the author highlighted the poor ROC result and attributed it to the effect of "neighboring yarns". Regardless of the discrepancy between that statement and the other statement "the fault can be detected with high confidence" (as tried to be explained in the caption of Figure 48), the size of the sub-window was not given for this particular case (it will be better to give this size than talking about an optical illusion of red and green colors in page 68). Also, it might be useful to show how changing the size of the sub-window may affect the ROC results.

Presenting the results in chapter 5 lacks the *deep discussions* and full of *redundant* figures. For example, if all samples were captured out of the same fabric (with the same structure), then most images given for the "*defect-free*" and their "*power spectra*" (images *a* and *c* in the second figure for each fault type) should be identical and no need to repeat them in each case. It might be useful, however, to indicate the *descriptor values* for the defect-free and the *deviation* from them in each case. This suggestion implies, for a good comparison, the need to use the same size of filters in all cases, and I suggest using a general "classifier" (with a suitable size of filters) at the end of chapter 5 to demonstrate the *performance* of this classifier with the different types of faults.

Finally, the conclusion of this study includes a few *alarming* statements that should be *reconsidered* by the author. One statement implies that: the author did not work *solely* on this research, and it came just as a byproduct of another system. The author also described the importance of the work as: the *detailed* discussions for *certain aspects* that usually *overlooked* by researchers in the textile field; however, this should maintain the *balance* with the topics of interest in that field (where the author is seeking a degree). It is not proper to *completely overlook* some important aspects in the presented research such as the fabric defects, technological reasons, and their impact on the quality of the product.





3 General comments

The *substantial* comments on the topic were given in the previous section of this report, however there are some *general* comments that are related to the overall dissertation and its style and formatting. These comments are listed below:

- The author used a reasonable English language in the dissertation. While there are some typos and grammar mistakes, they generally do not affect the meaning of the sentences and the context is still understandable. It is necessary, however, to proofread the dissertation again to correct these mistakes.
- The accuracy of detection is given by Equation (39), however the efficiency of detection is given in terms of TPR and FPR. There should be a consistency in the work, especially that the given "*efficiency*" sums up, in many cases, to values different than 100% (sometimes it is less than 100% and sometimes it is more).
- Since it is difficult for the reader to count all the "red" and "green" windows in each fault case, it will be more useful to add the "*confusion matrix*" next to each figure which will help in getting more grip of the numbers through the given discussions.
- It is understandable that DirectShow refers to its elements as "filters"; however, in this work I prefer to use the word "*module*" or "*node*" to refer to these elements and not to confuse it with the *filtration* process during the image analysis.
- Referring to the "*defect-free*" fabrics should not be with the words "*fine*" samples as noticed in chapter 5.
- The caption of Figure 8 refers to the origin as the point **O**, which should be corrected to the point *w* as given in the drawing.
- In Equation (37), it is better to use a different symbol other than Σ , just to avoid the confusion that might result from the special meaning of this symbol in mathematics.
- The page number of the "abbreviations" page (in the front-matter) is wrong and should be corrected (shown as page No. 4 then followed by page No. 1 in the introduction).
- All figures should be used in the main text with a referral and some comments. The following figures were not used in the text at all: Figures 22-23, 32, 43-44, 46-48, 51-52, and 55-64.
- All tables should be used in the main text with a referral and some comments. Table 1 should be used in page 52, for example: "...confusion matrix *given in Table 1*".

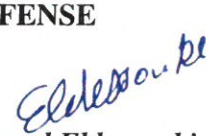


- All abbreviations should be clearly stated at their first appearance in the text. It is not enough to collect all abbreviations in a table at the beginning of the dissertation and leave them in the text without a clear description.
- The format of the biography should follow a *consistent style* and the names of all authors should appear (*according to the used style*, which also uses the abbreviation "*et al.*" only in the main body of the text).

4 Conclusion and Recommendations

The topic presented in this dissertation is very important for the scientific community and the methods implemented in this work were presented at a reasonable level. The problem solving approach in this work and its presentation were scientifically sound. On the other hand, the results presented in this dissertation are limited in scope and in significance, and the author should clarify some of the comments and questions highlighted in the discussion section of this report. The response for these comments is possible by correcting some sections of the dissertation according to the given guidelines, and therefore:

I RECOMMEND THIS WORK FOR A DEFENSE


Doc. Ing. Mohamed Eldessouki, PhD
Technical University of Liberec
Liberec. August 25, 2016



Oponentský posudek na disertační práci Ing. Jiřího Kuly

Automatic visual control system for textile processes (Automatická vizuální kontrola textilních procesů)

Předložená disertační práce se zabývá hardwarovou a softwarovou implementací systému pro on-line kontrolu kvality povrchové struktury textilie. Z tohoto hlediska se práce zabývá aktuální problematikou, jejíž řešení není v praktických provozech doposud uspokojivě vyřešeno.

Práce je formálně rozdělena do osmi kapitol a čtyř dodatků (které v obsahu na začátku práce nejsou uvedeny). Z věcného hlediska ji lze rozdělit na čtyři tématické části, jejichž popis řešení je uveden v kapitolách 2, 3 a 4. První částí je hardwarová implementace. Obsahuje velmi stručný popis zařízení, zkonstruovaného na katedře hodnocení textilií textilní fakulty TU Liberec (tato informace v textu opět chybí, stejně tak jako informace o autorech tohoto zařízení). Ve druhé části autor řeší problematiku získávání obrazu hodnocené textilie na daném zařízení. Této části je v práci věnována celá jedna kapitola (kapitola 2) a autor se zde zabývá transformací obrazu získaného při aplikaci dvou modelů: modelu centrální projekce (tzv. "pinhole camera") a modelu lineárního snímání (tzv. "line scan camera"). Velká část této teorie je převzata z literatury a autor se zde dopouští řady nepřesností ve vyjadřování (viz otázka 1). V závěru této kapitoly se autor věnuje původnímu řešení problému nezkresleného spojení dvou sousedních obrazů získaných ze dvou kamer, (jejich "narovnání"). Ve třetí části (v kapitole 4) disertant popisuje metodu zpracování získaného obrazu. K tomu používá diskrétní Fourierovu transformaci a Gáborovu filtraci. Na spektrální reprezentaci snímaného obrazu aplikuje sadu Gáborových filtrů, pro každý spočte dvě statistické charakteristiky. Tím dostane tzv. deskriptor daného obrazu. Vlastní detekce potom probíhá tak, že srovnává deskriptory získané při lineárním snímání s referenční hodnotou, získanou z pozorování nedefektní textilie. K tomu používá Hotellingovu T^2 statistiku. Součástí práce je ukázka výsledků této metodologie na různých typech vad textilie (v kapitole 5). Poslední čtvrtou částí je softwarová aplikace. Ta je popsána v kapitole 2 spolu s hardwarovou implementací. Z textu vyplývá, že program byl vyvíjen v jazycích C++ s využitím standardních knihoven. Softwarové řešení je modulární a otevřené k dalšímu rozšiřování.

Předložená práce je druhou přepracovanou verzí. Zatímco většině námitek k první verzi autor vyhověl a práce je na lepší úrovni, než byla původní verze, na hlavní otázku autor ani v této verzi jasně neodpověděl. Z práce jsem například nevyčetl, kdo je autorem návrhu zařízení pro snímání textilie, jaký je autorův podíl na konstrukci zařízení, na tvorbě software atd. V práci zůstala řada překlepů, které ovšem nemají vliv na obsah.

Otázky na disertanta:

- 1) Mohl by autor objasnit svá tvrzení na straně 19 před vzorcem (2)? Není jasné, jak je to s linearitou zobrazení "between three dimensional world points into two dimensional image points" vyjádřené rovnicí (2).
- 2) V kapitole 6 Conclusion (očekával bych spíše "Conclusions", neboť kapitola obsahuje více závěrů) autor mimo jiné uvádí, že "the weak part of the algorithm is the bank of filters itself" a o několik vět dále lze nalézt větu "Certainly the static bank of Gabor

filters is not the optimal solution". Jako alternativní řešení zde uvádí aplikaci neuronových sítí. Mohl by autor vysvětlit výhody a nevýhody použití Gáborovy filtrace ve srovnání s jinými metodami a objasnit, proč použil právě tuto metodu (když – podle jeho vlastních slov – není optimální)?

- 3) Hotellingova metoda srovnávání vícerozměrného pozorování s referenční hodnotou vyžaduje nějaké předpoklady pro její použití. Toto disertant ve své práci nijak nekomentuje a žádné předpoklady neověřuje. Při obhajobě by měl toto uvést na pravou míru.
- 4) Co je v této práci původním přínos autora k danému tématu? Přes moji výtku k první verzi této práce jsem ani v této přepracované verzi nenašel jasně vymezené původní výsledky práce disertanta a výsledky přejaté odjinud.

Disertant ve své práci nabízí řešení aktuální problematiky zpracování a analýzy obrazu v aplikaci na kontrolu kvality v textilní výrobě. V práci je použita poměrně složitá metodika pořizování a zpracování obrazové informace, založená na netriviální matematice. Není pochyb, že autor této metodice rozumí a dokáže ji aplikovat. Předloženou práci doporučuji k obhajobě.

Na závěr konstauji, že práce splňuje požadavky kladené na disertační práci a pokud autor uspokojivě zodpoví položené otázky, doporučuji udělení titulu PhD.

V Praze, dne 29. 9. 2016



prof. RNDr. Gejza Dohnal, CSc.